

Searching for neutrino electromagnetic properties with scattering experiments

Christoph Andreas Ternes

August 22nd 2026



**TWENTY-SECOND LOMONOSOV
CONFERENCE** August, 21-27, 2025
ON ELEMENTARY PARTICLE PHYSICS
MOSCOW STATE UNIVERSITY

Coherent elastic neutrino nucleus scattering

CEvNS was predicted in 1974!

PHYSICAL REVIEW D

VOLUME 9, NUMBER 5

1 MARCH 1974

Coherent effects of a weak neutral current

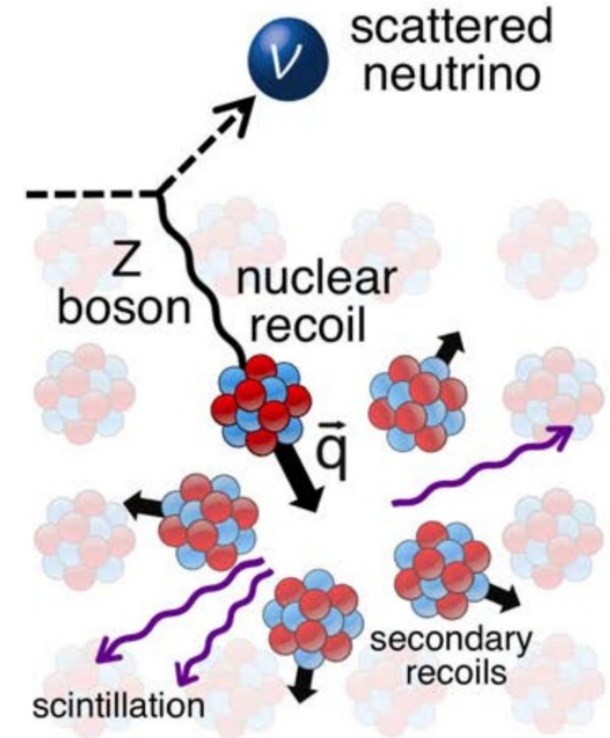
Daniel Z. Freedman†

National Accelerator Laboratory, Batavia, Illinois 60510

and Institute for Theoretical Physics, State University of New York, Stony Brook, New York 11790

(Received 15 October 1973; revised manuscript received 19 November 1973)

If there is a weak neutral current, then the elastic scattering process $\nu + A \rightarrow \nu + A$ should have a sharp coherent forward peak just as $e + A \rightarrow e + A$ does. Experiments to observe this peak can give important information on the isospin structure of the neutral current. The experiments are very difficult, although the estimated cross sections (about 10^{-38} cm^2 on carbon) are favorable. The coherent cross sections (in contrast to incoherent) are almost energy-independent. Therefore, energies as low as 100 MeV may be suitable. Quasi-coherent nuclear excitation processes $\nu + A \rightarrow \nu + A^*$ provide possible tests of the conservation of the weak neutral current. Because of strong coherent effects at very low energies, the nuclear elastic scattering process may be important in inhibiting cooling by neutrino emission in stellar collapse and neutron stars.



See the presentation by
A. Konovalov!!

Coherent elastic neutrino nucleus scattering

In the standard model we have

$$\frac{d\sigma_{\nu\ell-\mathcal{N}}}{dT_{\text{nr}}}(E, T_{\text{nr}}) = \frac{G_{\text{F}}^2 M}{\pi} \left(1 - \frac{MT_{\text{nr}}}{2E^2}\right) (Q_{\ell,\text{SM}}^V)^2$$

See the presentation by
A. Konovalov!!

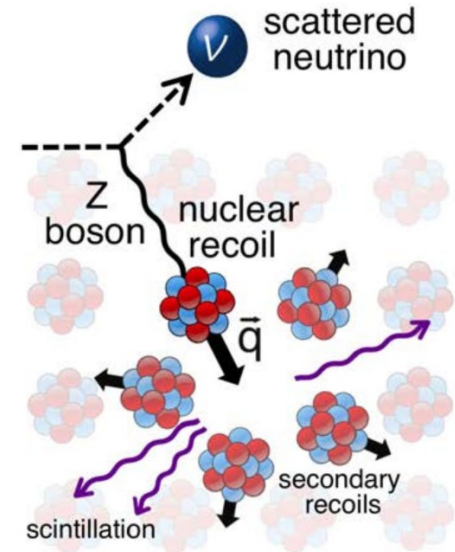
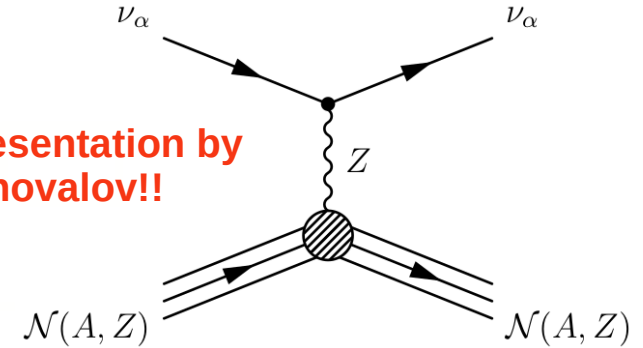
with the weak charge

$$Q_{\ell,\text{SM}}^V = \left[g_V^p(\nu_\ell) Z F_Z(|\vec{q}|^2) + g_V^n N F_N(|\vec{q}|^2) \right]$$

$$g_V^p(\nu_e) = 0.0401, \quad g_V^p(\nu_\mu) = 0.0318, \quad g_V^n = -0.5094$$

The cross section scales with the neutron number squared

The form factors describe the loss of coherence for large momentum transfer



Coherent elastic neutrino nucleus scattering

Measured at COHERENT:

- COH - CsI
- COH - Ar
- COH - Ge

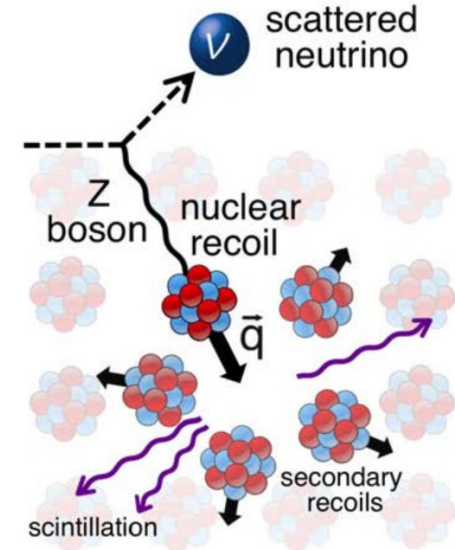
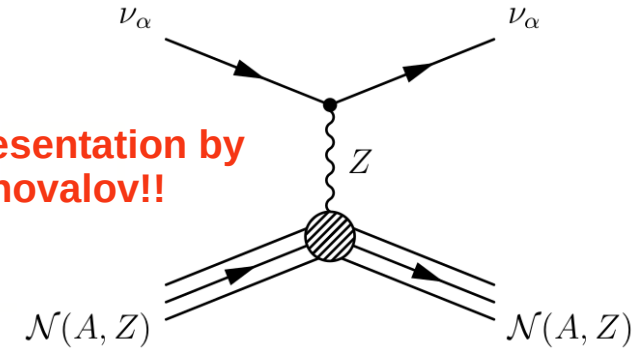
Measured at reactors:

- Dresden-II
- CONUS+

Measured at dark matter experiments

- PandaX-4T
- XENONnT

See the presentation by
A. Konovalov!!



Dark matter direct detection experiments

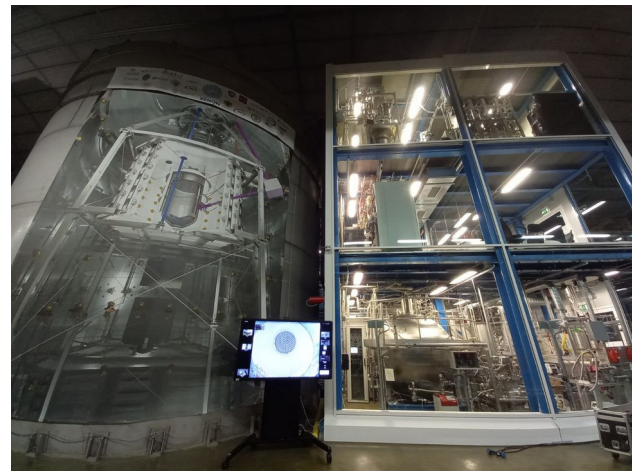
In addition to CEvNS, we will use data from several DMDD experiments

PandaX-4T (China)

LUX-ZEPLIN (USA)

XENONnT (Gran Sasso)

DARWIN (next generation experiment)



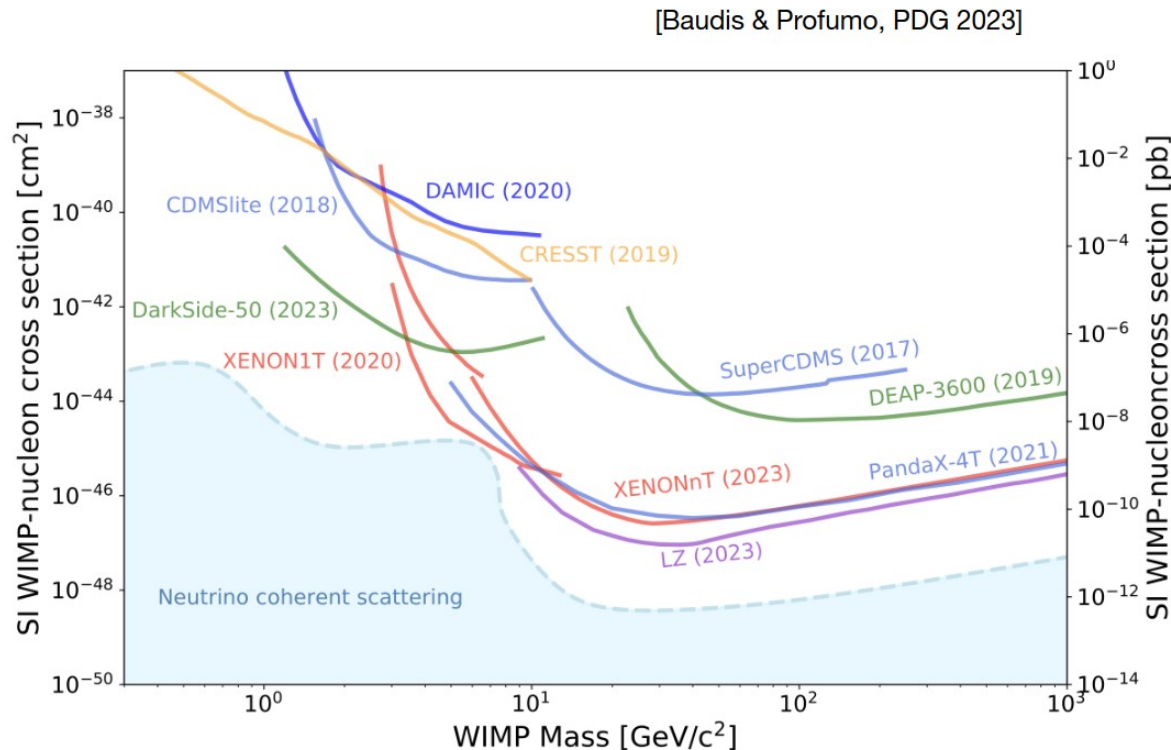
The original purpose of these experiments is to observe recoils induced by WIMP interactions

Solar neutrinos constitute an irreducible background for these experiments

These experiments can be used to measure nuclear and electron recoils!

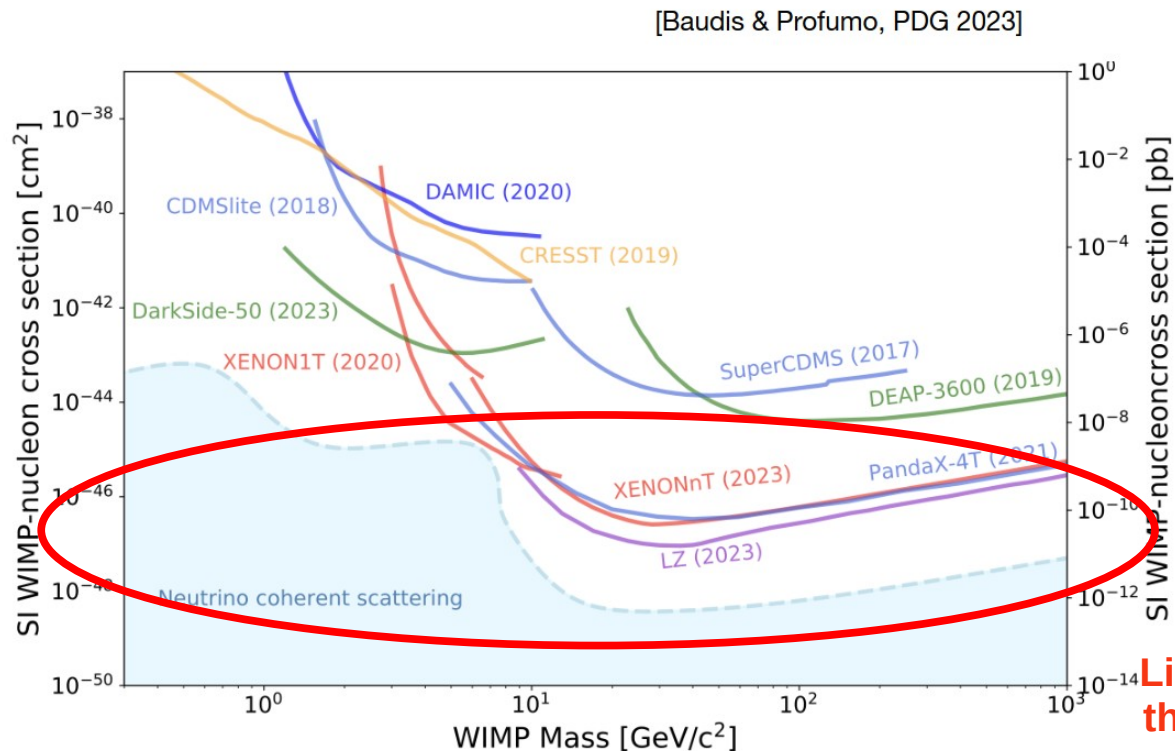
Dark matter direct detection experiments

Direct detection experiments put stringent bounds on the WIMP parameter space



Dark matter direct detection experiments

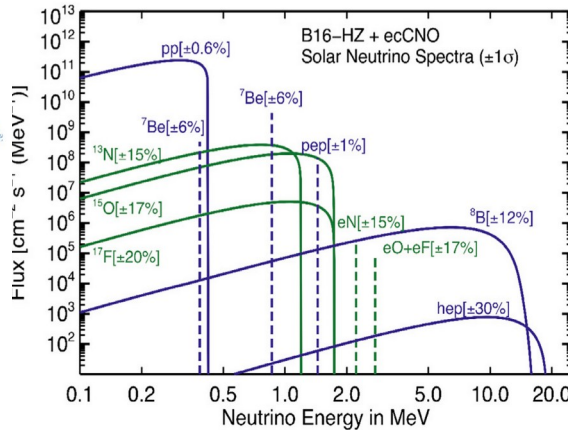
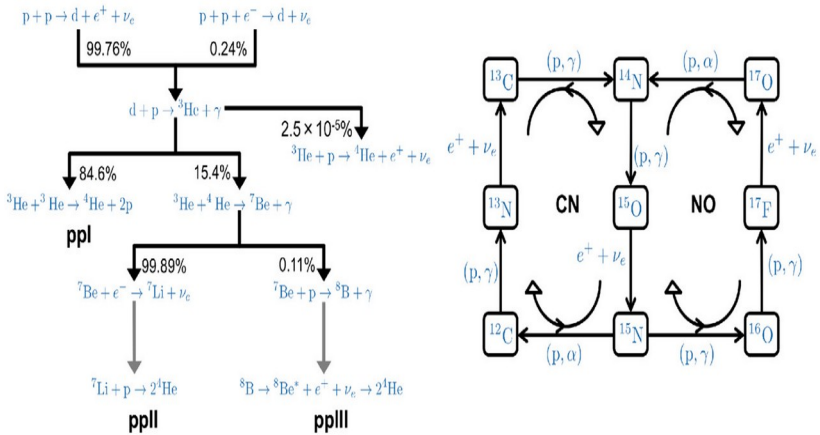
Direct detection experiments put stringent bounds on the WIMP parameter space



Limits are getting close to the so-called neutrino fog

Dark matter direct detection experiments

Solar neutrinos oscillate and arrive at a detector on Earth as a mixture of ν_e , ν_μ , and ν_τ , whose fluxes are given by

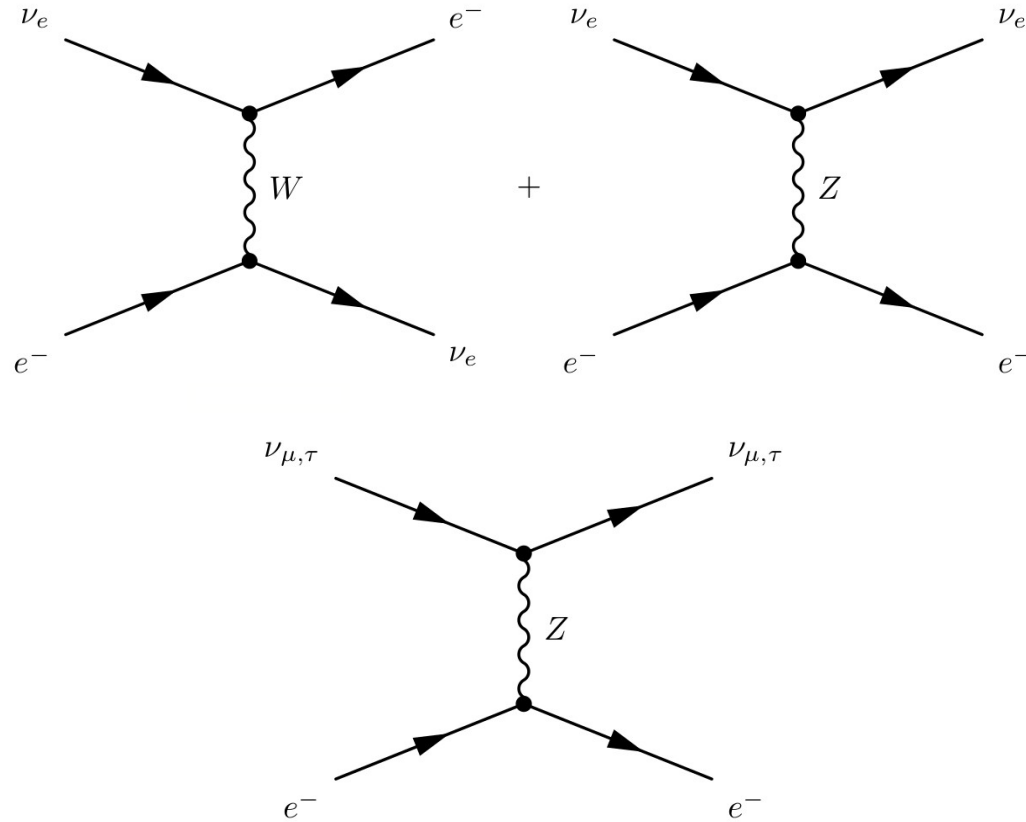


Flux	B16-HZ	B16-LZ
$\Phi(\text{pp})$	$5.98(1 \pm 0.006)$	$6.03(1 \pm 0.005)$
$\Phi(\text{pep})$	$1.44(1 \pm 0.01)$	$1.46(1 \pm 0.009)$
$\Phi(\text{hep})$	$7.98(1 \pm 0.30)$	$8.25(1 \pm 0.30)$
$\Phi(^7\text{Be})$	$4.93(1 \pm 0.06)$	$4.50(1 \pm 0.06)$
$\Phi(^8\text{B})$	$5.46(1 \pm 0.12)$	$4.50(1 \pm 0.12)$
$\Phi(^{13}\text{N})$	$2.78(1 \pm 0.15)$	$2.04(1 \pm 0.14)$
$\Phi(^{15}\text{O})$	$2.05(1 \pm 0.17)$	$1.44(1 \pm 0.16)$
$\Phi(^{17}\text{F})$	$5.29(1 \pm 0.20)$	$3.26(1 \pm 0.18)$
$\Phi(\text{eN})$	$2.20(1 \pm 0.15)$	$1.61(1 \pm 0.14)$
$\Phi(\text{eO})$	$0.81(1 \pm 0.17)$	$0.57(1 \pm 0.16)$
$\Phi(\text{eF})$	$3.11(1 \pm 0.20)$	$1.91(1 \pm 0.18)$

$$\Phi_{\nu_e}^i = \Phi_{\nu_e}^{i\odot} P_{ee}, \quad \Phi_{\nu_\mu}^i = \Phi_{\nu_e}^{i\odot} (1 - P_{ee}) \cos^2 \vartheta_{23}, \quad \Phi_{\nu_\tau}^i = \Phi_{\nu_e}^{i\odot} (1 - P_{ee}) \sin^2 \vartheta_{23}$$

Villante, Serenelli, 2101.03077, Frontiers 2021

Elastic neutrino electron scattering



Elastic neutrino electron scattering

In the standard model we have

$$\frac{d\sigma_{\nu_\ell\text{-Xe}}^{\text{SM}}}{dT_e}(E_\nu, T_e) = Z_{\text{eff}}^{\text{Xe}}(T_e) \frac{G_F^2 m_e}{2\pi} \left[(g_V^{\nu_\ell} + g_A^{\nu_\ell})^2 + (g_V^{\nu_\ell} - g_A^{\nu_\ell})^2 \left(1 - \frac{T_e}{E_\nu}\right)^2 - ((g_V^{\nu_\ell})^2 - (g_A^{\nu_\ell})^2) \frac{m_e T_e}{E_\nu^2} \right]$$

with the couplings

$$g_V^{\nu_e} = 2 \sin^2 \vartheta_W + 1/2,$$

$$g_A^{\nu_e} = 1/2,$$

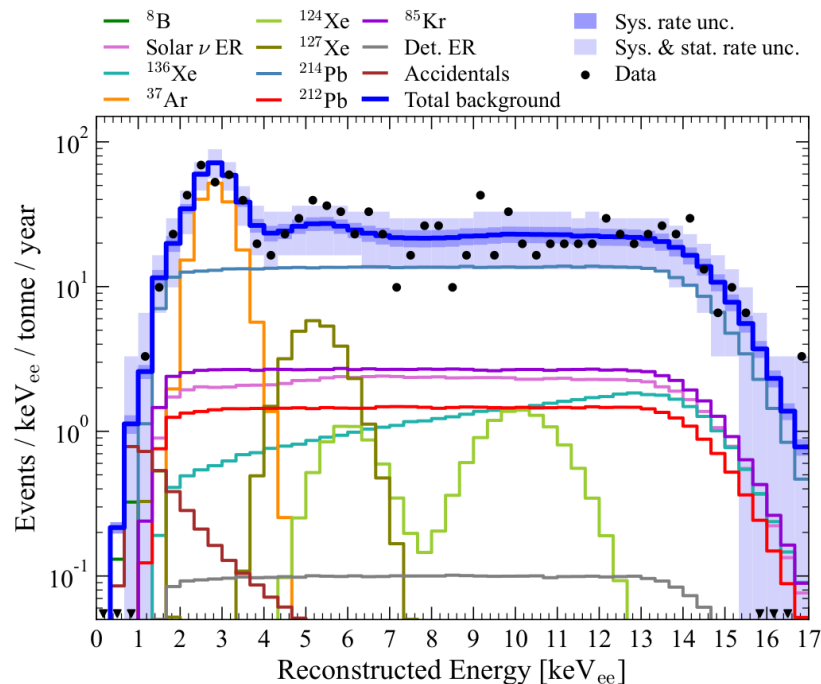
$$g_V^{\nu_{\mu,\tau}} = 2 \sin^2 \vartheta_W - 1/2,$$

$$g_A^{\nu_{\mu,\tau}} = -1/2,$$

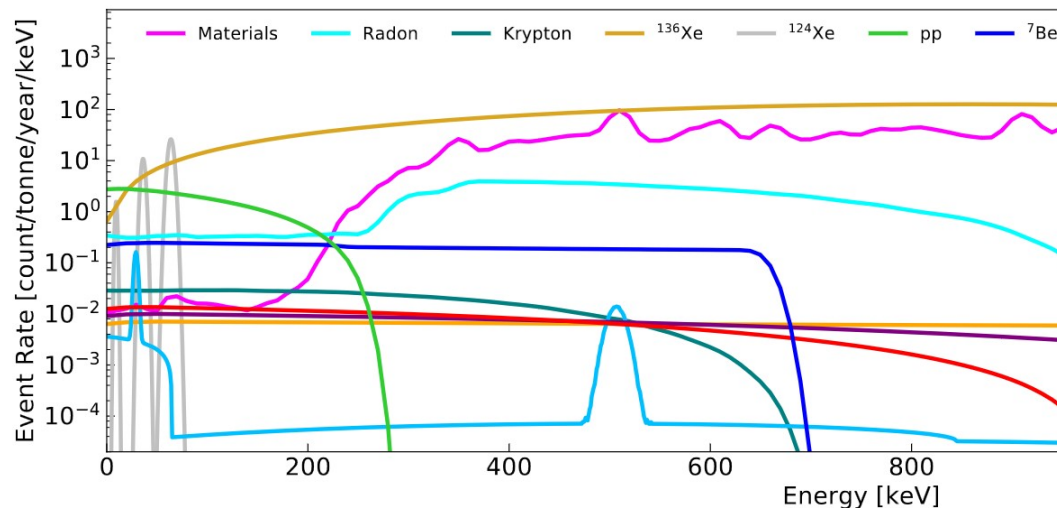
The first factor quantifies the effective number of electrons which can be ionized for a given recoil energy

Dark matter direct detection experiments

Solar neutrino EvES constitutes a subdominating (dominating) background component in current (future) experiments

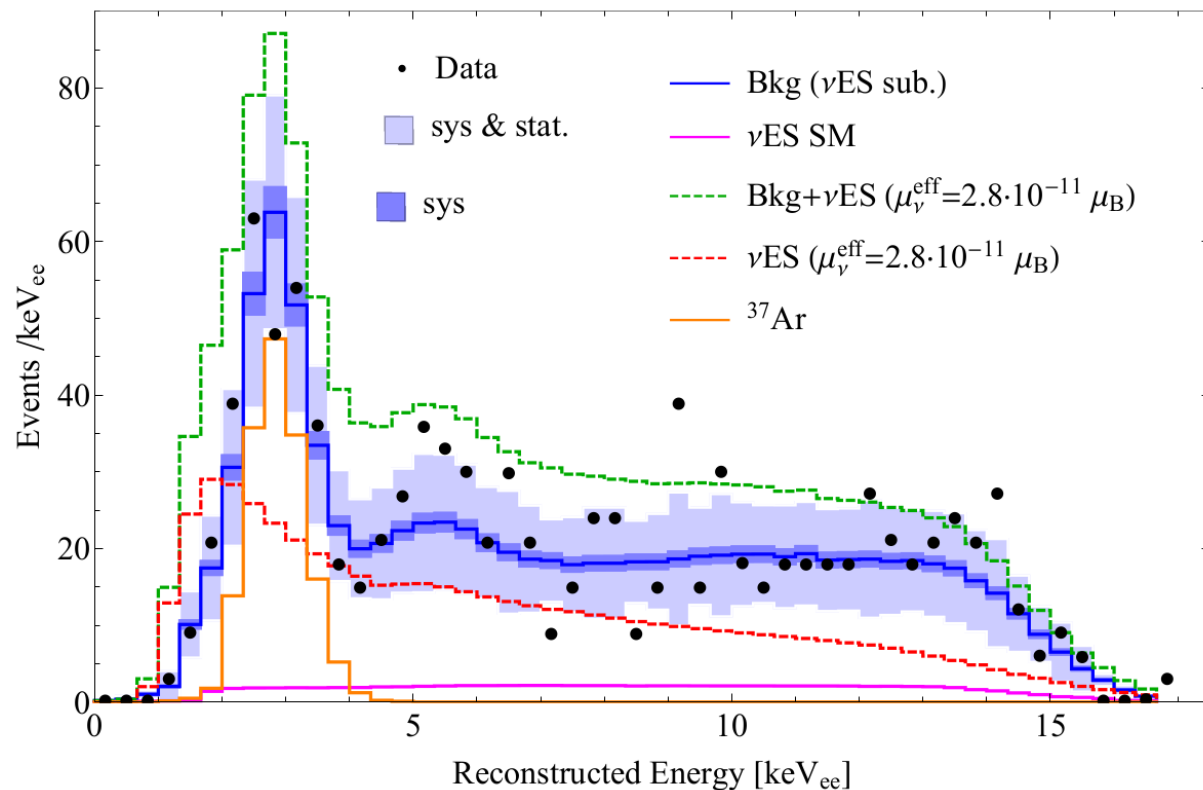


LZ, 2211.17120, PRD 2023



DARWIN, 2006.03114, EPJC 2020

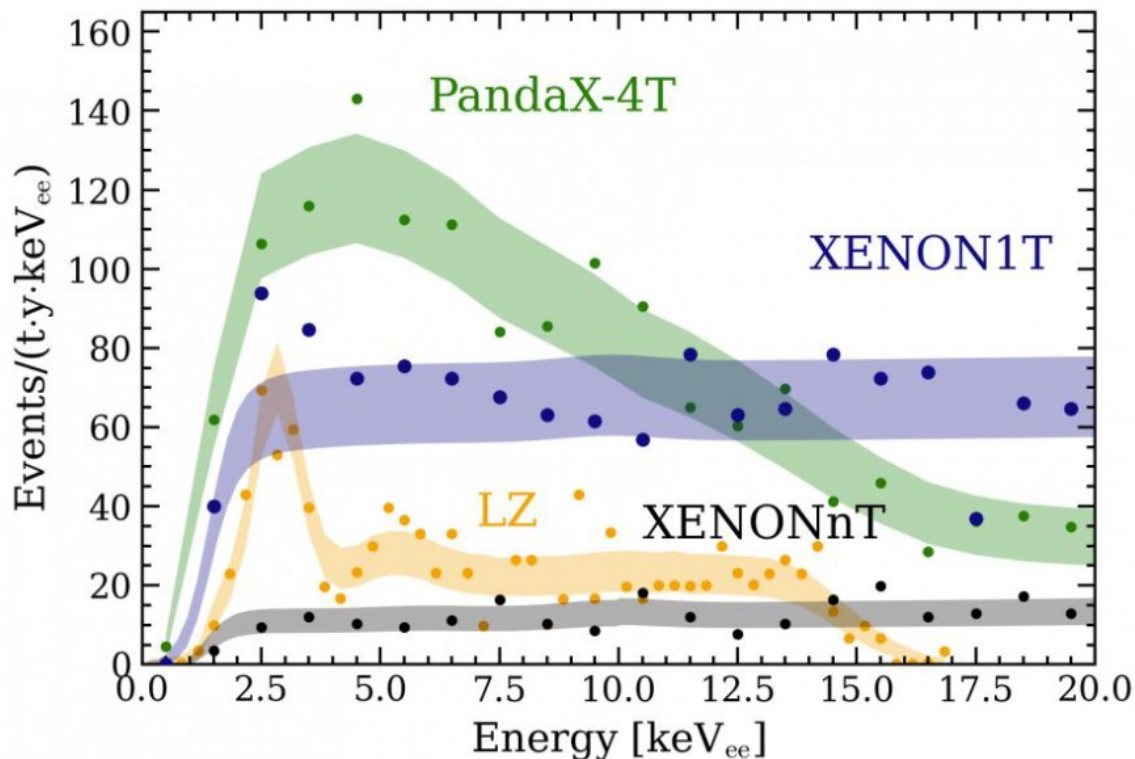
Dark matter direct detection experiments



Even though the EvES rate is very small in the SM, new physics can dramatically increase the cross section

Atzori Corona et al, 2207.05036, PRD 2023

Dark matter direct detection experiments



XENONnT has the lowest background rate

We can expect the strongest constraints on new physics from XENONnT data

PandaX-4T, 2206.02339, PRL 2022

LZ, 2207.03764, PRL 2023

XENON, 2207.11330, PRL2022

Dark matter direct detection experiments

Again all background components with systematical uncertainties must be taken into account

$$R_k^X = R_k^{E\nu ES} + \sum_i R_k^i \quad R_k^{E\nu ES} = N \int_{T_e^k}^{T_e^{k+1}} dT_e \int_0^\infty dT'_e R(T_e, T'_e) A(T'_e) \sum_{i=pp, {}^7\text{Be}} \int_{E_\nu^{\min}}^{E_{\nu,i}^{\max}} dE_\nu \sum_\ell \Phi_{\nu_\ell}^i(E_\nu) \frac{d\sigma_{\nu_\ell}}{dT'_e}$$

$$\chi_X^2 = \min_{\vec{\alpha}, \vec{\beta}} \left\{ 2 \left(\sum_k R_k^X - D_k^X + D_k^X \log D_k^X / R_k^X \right) + \sum_i (\alpha_i / \sigma_{\alpha_i})^2 + \sum_i (\beta_i / \sigma_{\beta_i})^2 \right\}$$

We also perform a combined analysis of all DMDD experiments considering possible correlations among systematic uncertainties

Possible new physics contributions

Scattering can be altered by many BSM scenarios (similar for EvES)

See the related talks by

Y. Farzan

A. Konovalov

K. Kouzakov

D. Medvedev

S. Zavatarelli

G. Li

A. Shakirov

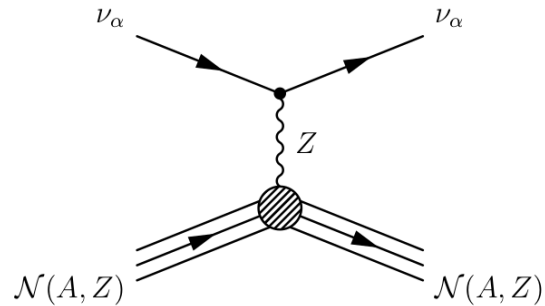
M. Mustamin

P. Denton

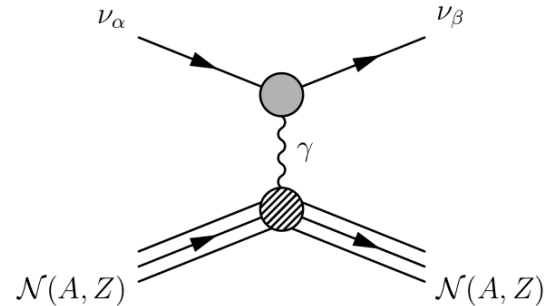
M. Demirci

O. Basli

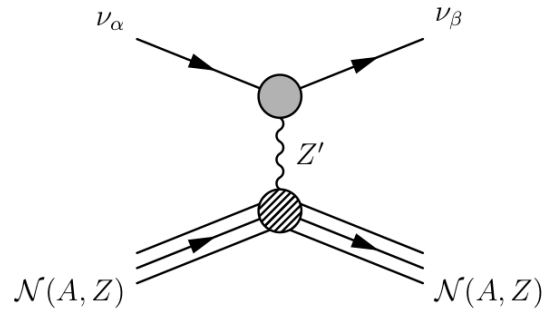
Standard Model NC



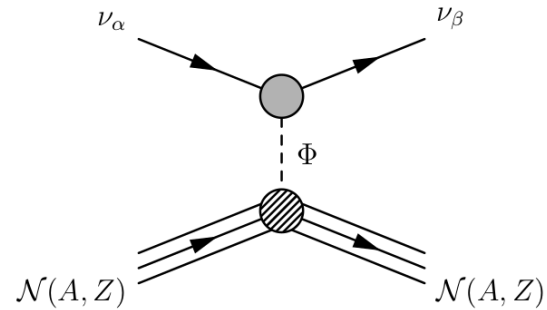
Electromagnetic Interactions



BSM Vector Mediator

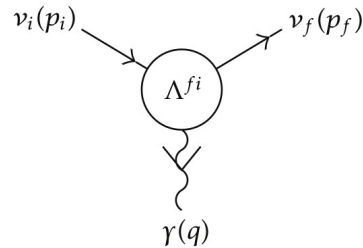


BSM Scalar Mediator



Neutrino electromagnetic interactions

$$\mathcal{H}_{\text{em}}^{(\nu)} = j_{\lambda}^{(\nu)} A^{\lambda} = \sum_{j,k=1}^3 \bar{\nu}_j \Lambda_{\lambda}^{jk} \nu_k A^{\lambda}$$



In some extensions of the Standard Model neutrinos acquire also electromagnetic properties through quantum loops effects

$$\Lambda_{\lambda}(q) = \left(\gamma_{\lambda} - \frac{q_{\lambda} \not{q}}{q^2} \right) [f_Q(q^2) + f_A(q^2) q^2 \gamma^5] - i \sigma_{\lambda\rho} q^{\rho} [f_M(q^2) + i f_E(q^2) \gamma^5]$$

Neutrino charge

Anapole

Magnetic and electric moments

See:

Giunti, Studenikin, 1403.6344, Rev.Mod.Phys 2015

Giunti, Kouzakov, Li, Studenikin, 2411.03122

Kouzakov, Studenikin, 1703.00401, PRD 2017

Neutrino magnetic moments

In the minimal extended SM the magnetic moment is strongly suppressed by the small size of the neutrino mass

$$\mu_\nu = \frac{3eG_F}{8\sqrt{2}\pi^2} m_\nu \simeq 3.2 \times 10^{-19} \left(\frac{m_\nu}{\text{eV}} \right) \mu_B$$

However, more complex models allow for larger magnetic moments, e.g. in left-right symmetric models

$$\mu_{\nu_l} = \frac{eG_F}{2\sqrt{2}\pi^2} \left[m_l \left(1 - \frac{m_{W_1}^2}{m_{W_2}^2} \right) \sin 2\xi + \frac{3}{4} m_{\nu_l} \left(1 + \frac{m_{W_1}^2}{m_{W_2}^2} \right) \right]$$

See Brogini, Giunti, Studenikin, 1207.3980, Adv.HEP 2012

Neutrino magnetic moments

Neutrino magnetic and electric dipoles contribute to CEvNS and EvES

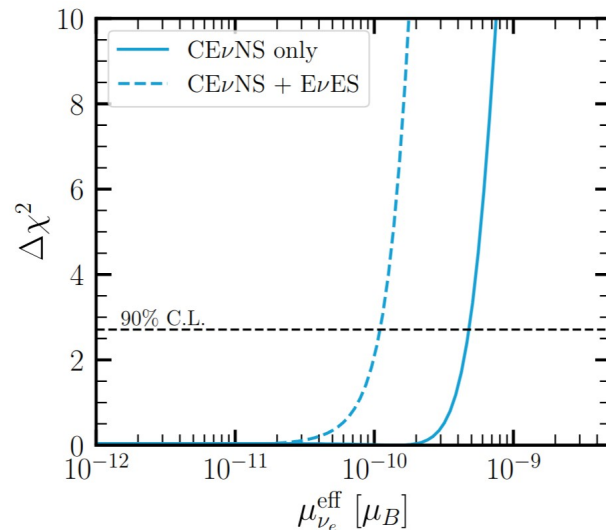
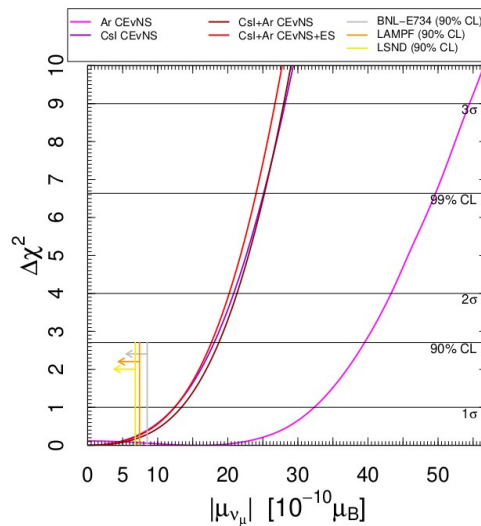
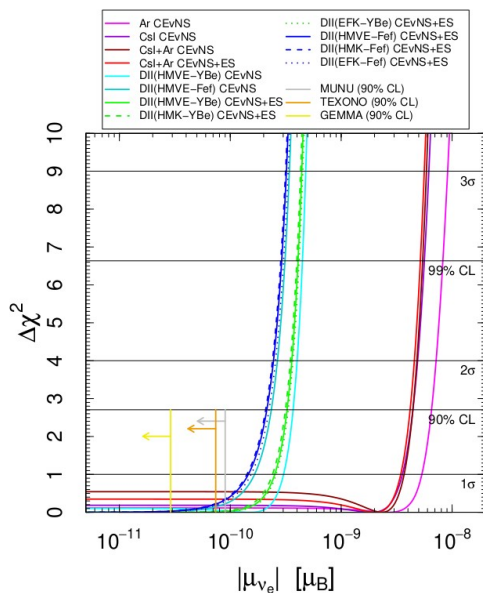
The magnetic moment interaction adds incoherently to the weak interaction because it flips helicity

$$\frac{d\sigma_{\nu\ell-\mathcal{N}}^{\text{MM}}(E, T_{\text{nr}})}{dT_{\text{nr}}} = \frac{\pi\alpha^2}{m_e^2} \left(\frac{1}{T_{\text{nr}}} - \frac{1}{E} \right) Z^2 F_Z^2(|\vec{q}|^2) \left| \frac{\mu_{\nu\ell}}{\mu_B} \right|^2$$

$$\frac{d\sigma_{\nu\ell-\mathcal{A}}^{\text{ES, MM}}(E, T_e)}{dT_e} = Z_{\text{eff}}^{\mathcal{A}}(T_e) \frac{\pi\alpha^2}{m_e^2} \left(\frac{1}{T_e} - \frac{1}{E} \right) \left| \frac{\mu_{\nu\ell}}{\mu_B} \right|^2$$

Vogel, Engel, PRD 1989

Neutrino magnetic moments



Atzori Corona, et al, 2205.09484, JHEP 2022

See also: De Romeri et al, 2211.11905, JHEP 2023

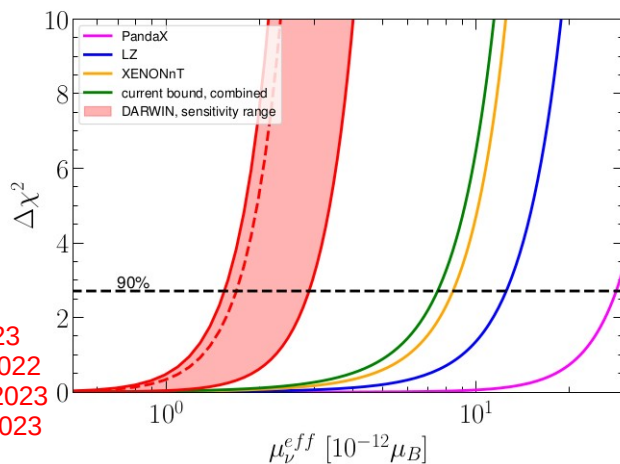
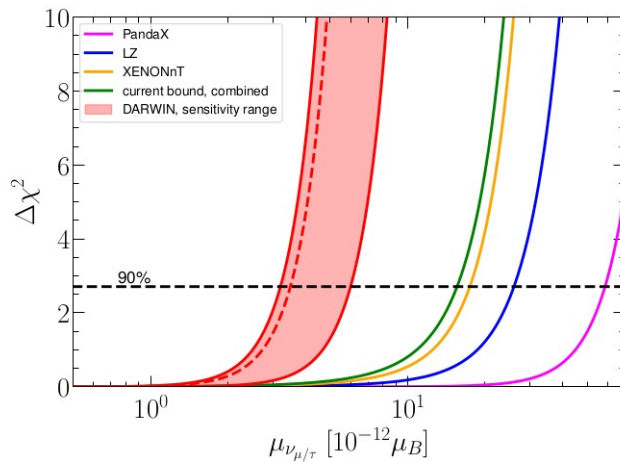
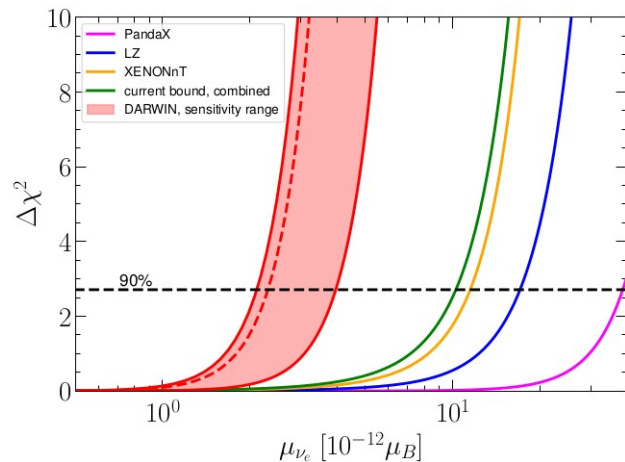
De Romeri et al, 2501.17843, PRD 2025

See also: Atzori Corona et al, 2501.18550, PRD 2025

COHERENT and reactor data can be used to place bounds on the electron and muon sector

CEvNS bounds are not yet competitive with bounds from other probes

Neutrino magnetic moments



DMDD can be used to place bounds also on the tau sector

These are the strongest laboratory bounds on neutrino magnetic moments

DARWIN will improve these bounds by up to a factor of 5

Giunti, Ternes, 2309.17380, PRD 2023
See also: XENON, 2207.11330, PRL 2022
Atzori Corona et al, 2207.05036, PRD 2023
ShivaSankar, et al, 2208.06415, PLB 2023

Neutrino magnetic moments

Giunti, Ternes, 2309.17380, PRD 2023

$(\Delta\chi^2 = 2.71)$

Experiment	$ \mu_{\nu_e} \ [10^{-12}\mu_B]$	$ \mu_{\nu_{\mu/\tau}} \ [10^{-12}\mu_B]$	$ \mu_{\nu}^{eff} \ [10^{-12}\mu_B]$
PandaX-4T	< 38.7	< 58.6	< 28.3
LZ	< 17.1	< 25.9	< 12.5
XENONnT	< 11.5	< 17.5	< 8.4
combined	< 10.3	< 15.6	< 7.5
DARWIN 30 ty	< 4.0	< 6.0	< 2.9
DARWIN 300 ty	< 2.3	< 3.5	< 1.7
DARWIN 300 ty depl.	< 2.1	< 3.2	< 1.5

DMDD bounds are stronger than BOREXINO bounds:

$$\Delta\chi^2 = 1.64 \quad \mu_{\nu_e} < 3.7 \times 10^{-11} \mu_B, \quad \mu_{\nu_{\mu}} < 5.0 \times 10^{-11} \mu_B, \quad \mu_{\nu_{\tau}} < 5.9 \times 10^{-11} \mu_B$$

DARWIN would become competitive with astrophysical observations

$$\mu_{\nu} < 1.5 \times 10^{-12} \mu_B \ (95\% \text{ CL})$$

Coloma et al, 2204.03011, JHEP 2022

Capozzi, Raffelt, 2007.03694, PRD 2020

Comparing neutrino magnetic moments

The effective (!) magnetic moment measured at different types of experiments is not the same!

The effective magnetic moments depend on the underlying fundamental dipole moments, neutrino mixing parameters and others

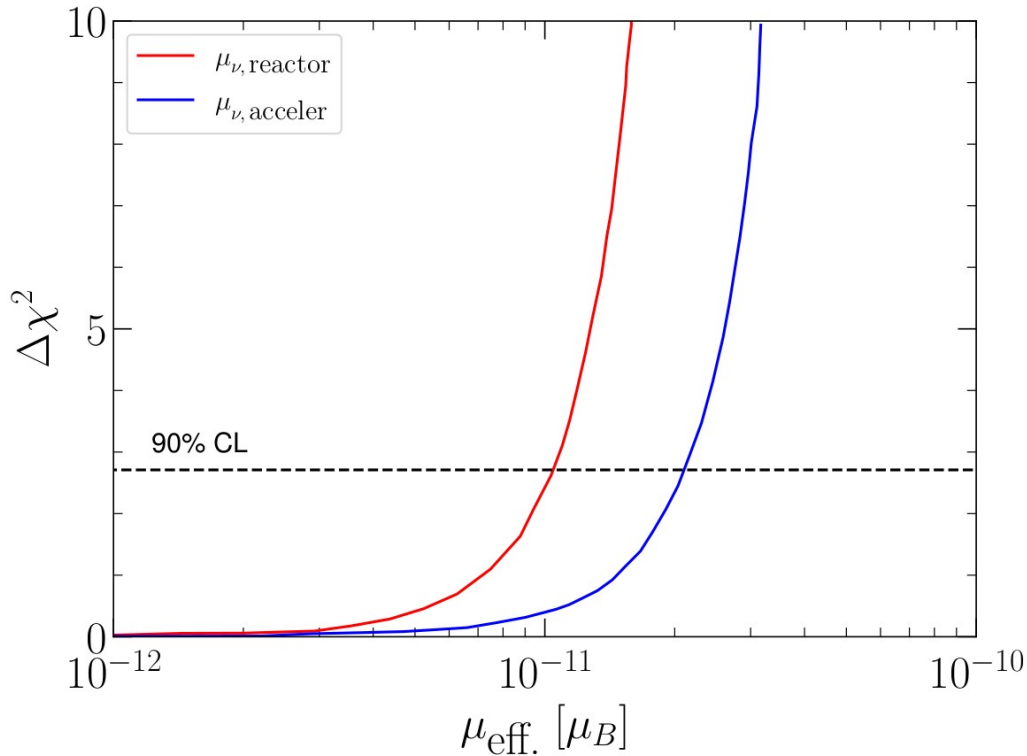
E.g. for solar neutrinos one has

$$(\mu_{\text{sol}}^M)^2 = |\mathbf{\Lambda}|^2 - c_{13}^2 |\Lambda_2|^2 + (c_{13}^2 - 1) |\Lambda_3|^2 + c_{13}^2 P_{e1}^{2\nu} (|\Lambda_2|^2 - |\Lambda_1|^2)$$

whereas for (short-baseline) reactors we find

$$\begin{aligned} (\mu_R^M)^2 &= |\mathbf{\Lambda}|^2 - s_{12}^2 c_{13}^2 |\Lambda_2|^2 - c_{12}^2 c_{13}^2 |\Lambda_1|^2 - s_{13}^2 |\Lambda_3|^2 \\ &\quad - 2s_{12}c_{12}c_{13}^2 |\Lambda_1| |\Lambda_2| \cos \delta_{12} - 2c_{12}c_{13}s_{13} |\Lambda_1| |\Lambda_3| \cos \delta_{13} \\ &\quad - 2s_{12}c_{13}s_{13} |\Lambda_2| |\Lambda_3| \cos \delta_{23} \end{aligned}$$

Comparing neutrino magnetic moments



Ternes, Tortola, 2505.02633

We translated the strongest bounds on the fundamental (!) moments (from DMDD data) into the relevant bounds for reactor and accelerator neutrinos:

$$\mu_{\nu, \text{reactor}} < 1.0 \times 10^{-11} \mu_B$$

$$\mu_{\nu, \text{acceler}} < 2.1 \times 10^{-11} \mu_B$$

Future experiments must improve over these numbers, not the effective magnetic moment directly obtained from DMDD

$$\mu_{\text{sol}} < 7.5 \times 10^{-12} \mu_B$$

Sterile dipole portal

Scattering of an active neutrino into a heavy sterile neutrino

$$\mathcal{L}_{\text{DP}} = \bar{N}_4(i\not{\partial} - m_4)N_4 + \frac{\sqrt{\pi\alpha_{\text{EM}}}}{2m_e} \left| \frac{\mu_{\nu_\ell}}{\mu_B} \right|^2 \bar{N}_4 \sigma_{\mu\nu} \nu_\ell F^{\mu\nu}$$

Cross section becomes identical to magnetic moment for tiny masses

$$\begin{aligned} \left. \frac{d\sigma_{\nu_\ell \mathcal{N}}}{dT_{\mathcal{N}}} \right|_{\text{DP}} &= \frac{\pi\alpha_{\text{EM}}^2}{m_e^2} Z^2 F_W^2(|\mathbf{q}|^2) \left| \frac{\mu_{\nu_\ell}}{\mu_B} \right|^2 \\ &\times \left[\frac{1}{T_{\mathcal{N}}} - \frac{1}{E_\nu} - \frac{m_4^2}{2E_\nu T_{\mathcal{N}} m_{\mathcal{N}}} \left(1 - \frac{T_{\mathcal{N}}}{2E_\nu} + \frac{m_{\mathcal{N}}}{2E_\nu} \right) + \frac{m_4^4(T_{\mathcal{N}} - m_{\mathcal{N}})}{8E_\nu^2 T_{\mathcal{N}}^2 m_{\mathcal{N}}^2} \right] \end{aligned}$$

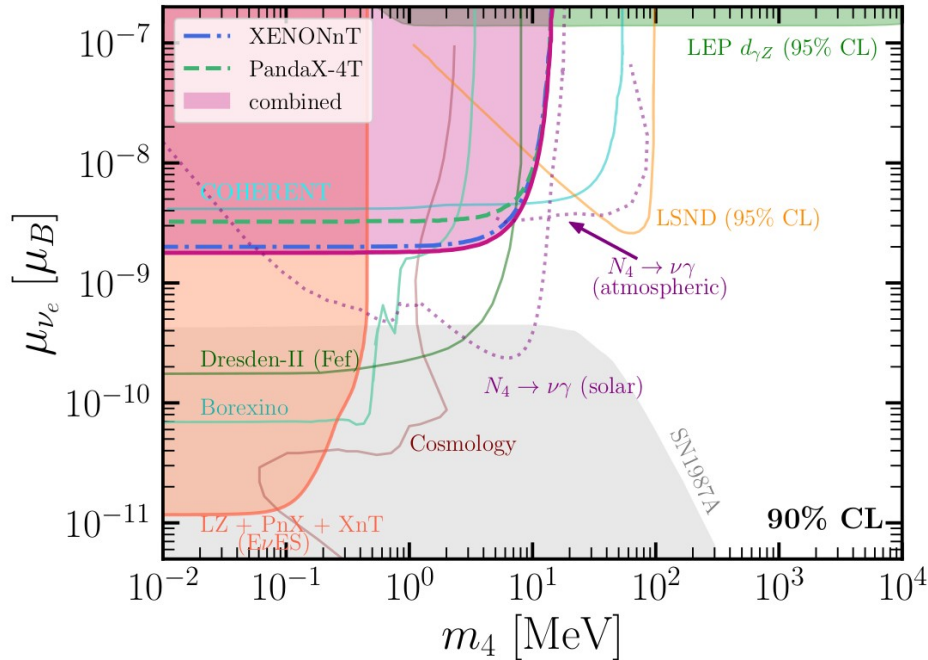
Gninenko, Krasnikov, hep-ph/9808370, PLB 1999

Grimus, Schwetz, hep-ph/0006028, NPB 2000

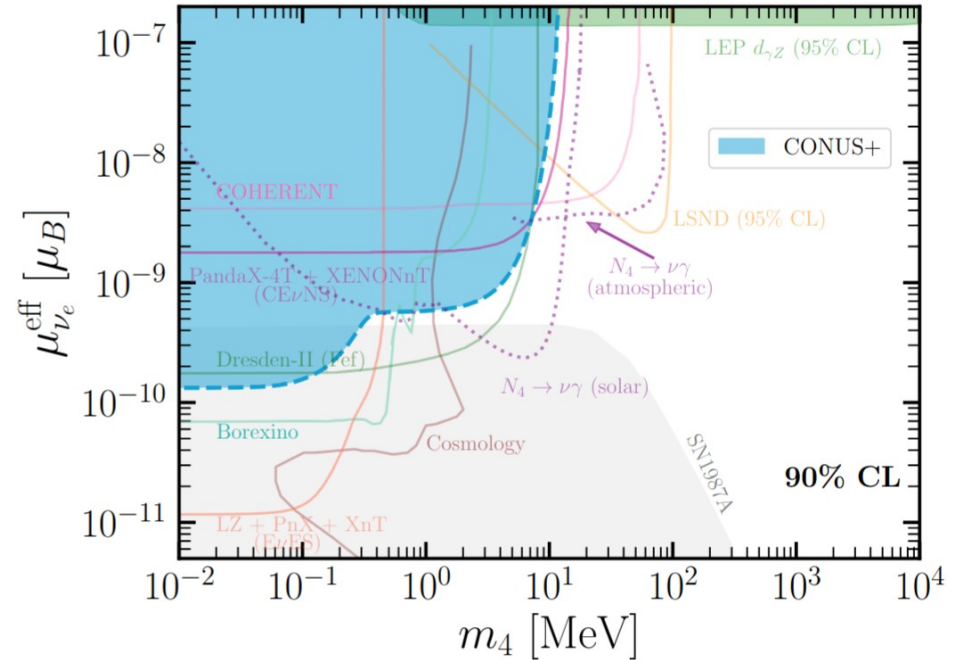
McKeen, Pospelov, 1011.3046, PRD 2010

Sterile dipole portal

Complementary bounds from scattering experiments



De Romeri et al, 2412.14991, JCAP 2025



De Romeri et al, 2501.17843, PRD 2025

Neutrino millicharges

In some BSM theories neutrinos may acquire small electric charges

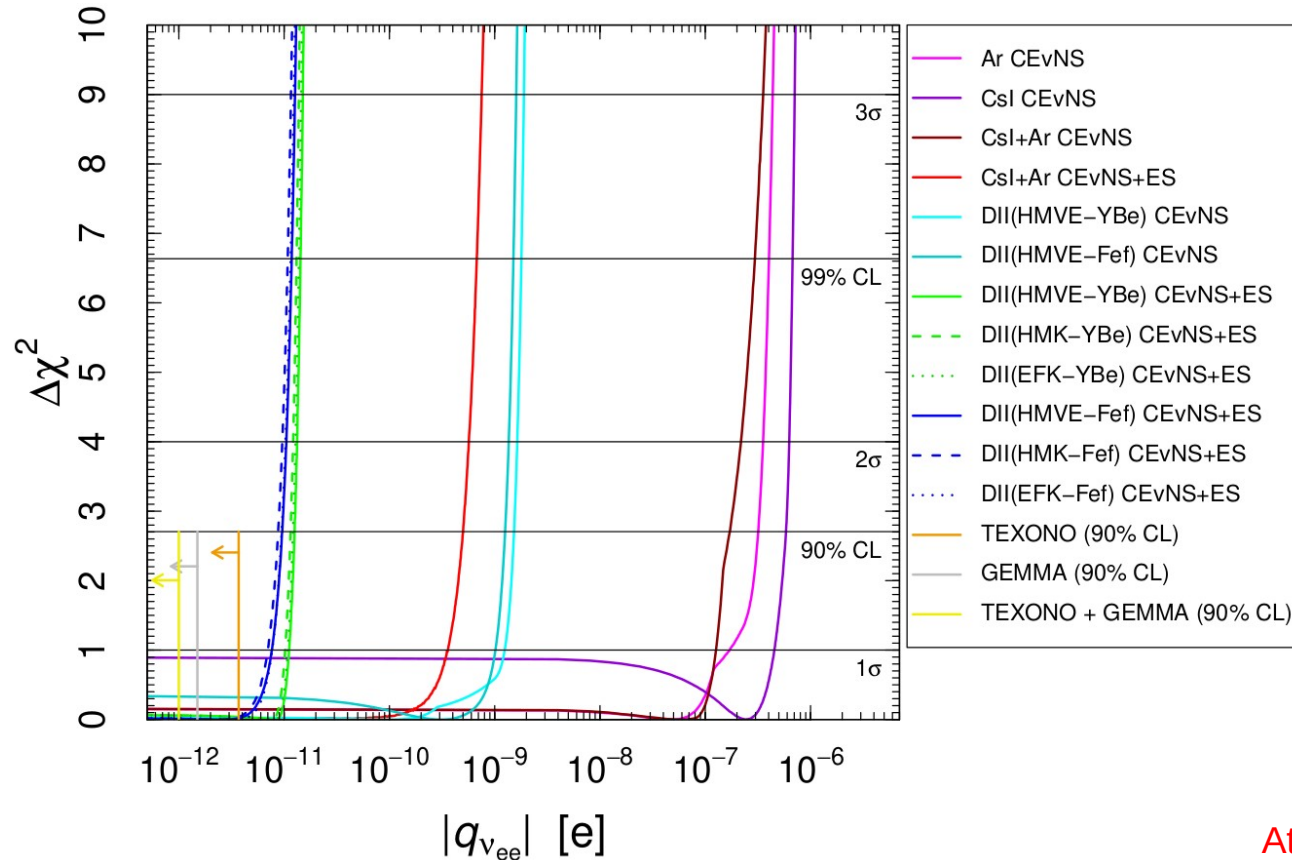
The cross section receives extra contributions which add coherently (diagonal charges) and incoherently (non-diagonal charges) to the SM cross section

$$\frac{d\sigma_{\nu_\ell - \text{Xe}}^{\text{SM}+\text{EC}}}{dT_e} = \left(\frac{d\sigma_{\nu_\ell - \text{Xe}}^{\text{SM}+\text{EC}}}{dT_e} \right)_{q_{\nu_\ell}} + \sum_{\ell' \neq \ell} \left(\frac{d\sigma_{\nu_\ell - \text{Xe}}^{\text{EC}}}{dT_e} \right)_{q_{\nu_{\ell\ell'}}$$

$$g_V^{\nu_\ell} \rightarrow g_V^{\nu_\ell} - \frac{\sqrt{2}\pi\alpha}{G_F m_e T_e} q_{\nu_\ell}$$

$$\left(\frac{d\sigma_{\nu_\ell - \text{Xe}}^{\text{EC}}}{dT_e} \right)_{q_{\nu_{\ell\ell'}}} = Z_{\text{eff}}^{\text{Xe}}(T_e) \frac{\pi\alpha^2}{m_e T_e^2} \left[1 + \left(1 - \frac{T_e}{E_\nu} \right)^2 - \frac{m_e T_e}{E_\nu^2} \right] |q_{\nu_{\ell\ell'}}|^2$$

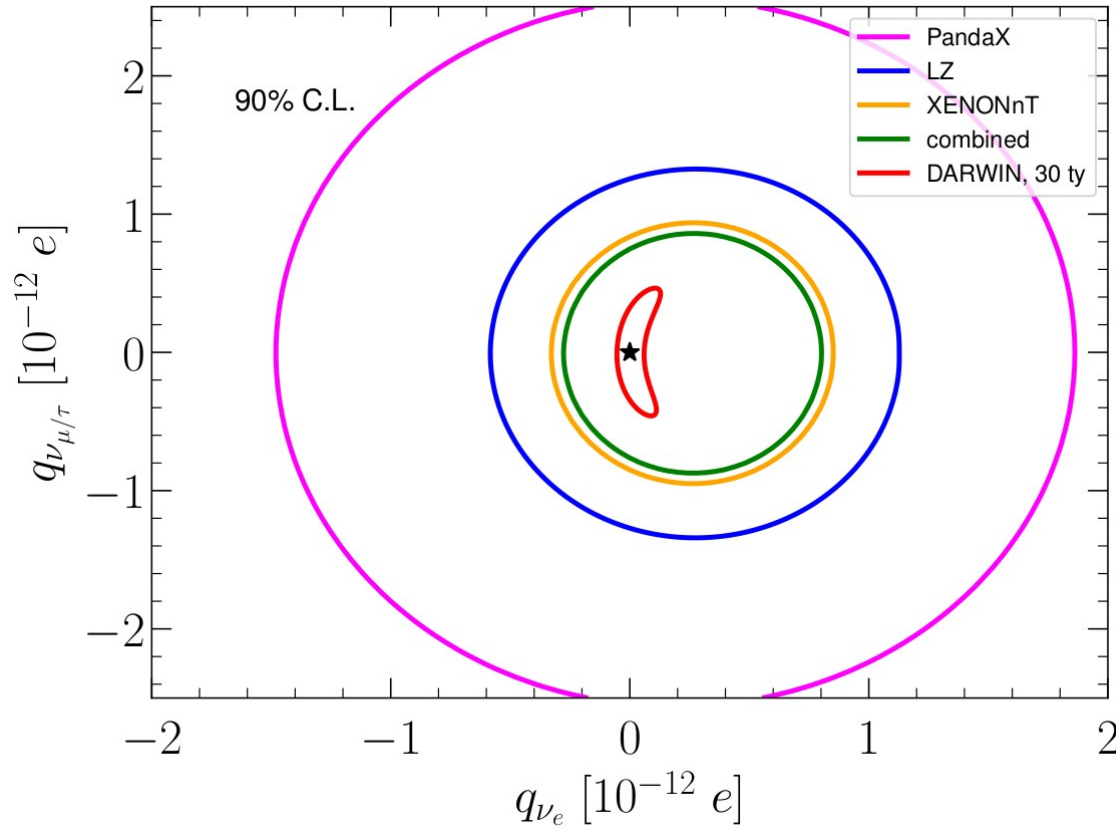
Neutrino millicharges



As previously, bounds from CEvNS experiments are not yet competitive with bounds from other experiments (Similar strength for other charges)

Atzori Corona et al, 2205.09484, JHEP 2022
See also: De Romeri et al, 2211.11905, JHEP 2023

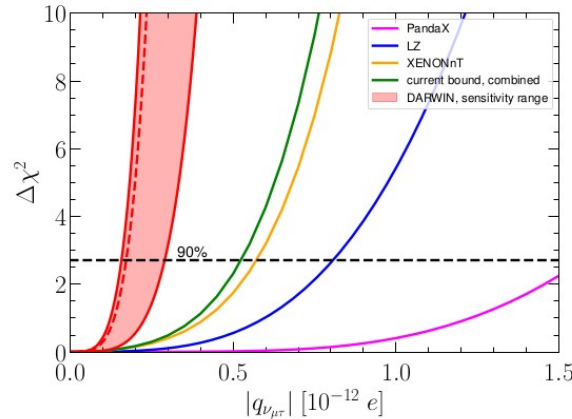
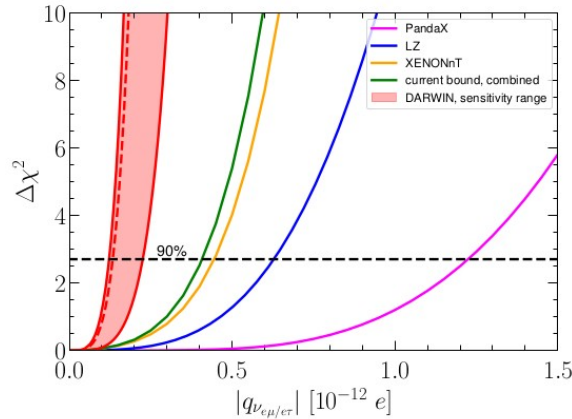
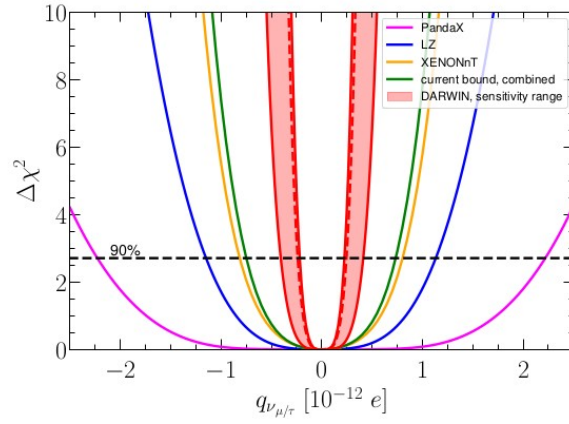
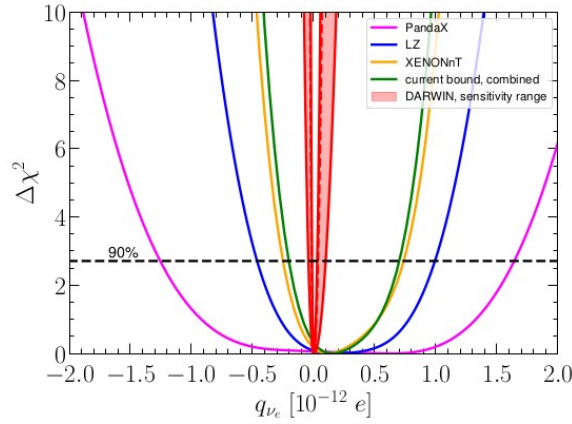
Neutrino millicharges



We obtain very strong bounds from DMDD experiments

Cancellations among parameters can occur and must be taken into account when deriving bounds

Neutrino millicharges



We obtain very strong bounds from DMDD experiments

Cancellations among parameters can occur and must be taken into account when deriving bounds

Bounds can be significantly improved by DARWIN

Neutrino millicharges

DMDD bounds are around 3 orders of magnitude more stringent than COHERENT bounds

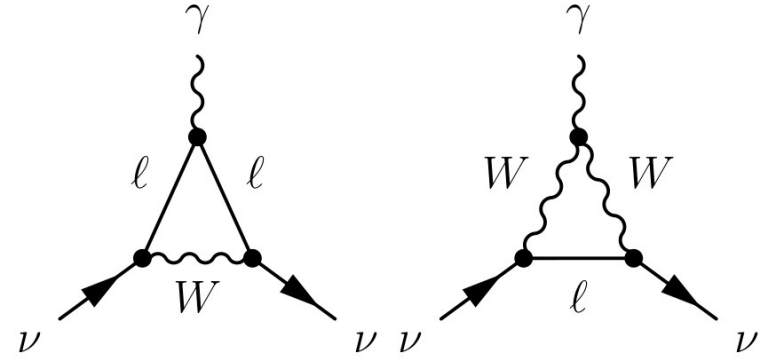
	CsI (CEvNS+ES) + Ar (CEvNS)			
$q_{\nu_{ee}}$	$(-3.5, 3.5) \times 10^{-10}$	$(-5.0, 5.0) \times 10^{-10}$	$(-5.6, 5.6) \times 10^{-10}$	$(-7.5, 7.5) \times 10^{-10}$
$q_{\nu_{\mu\mu}}$	$(-1.2, 1.2) \times 10^{-10}$	$(-1.9, 1.9) \times 10^{-10}$	$(-2.2, 2.2) \times 10^{-10}$	$(-3.2, 3.2) \times 10^{-10}$
$ q_{\nu_{e\mu}} $	$< 1.2 \times 10^{-10}$	$< 1.8 \times 10^{-10}$	$< 2.2 \times 10^{-10}$	$< 3.1 \times 10^{-10}$
$ q_{\nu_{e\tau}} $	$< 3.6 \times 10^{-10}$	$< 5.0 \times 10^{-10}$	$< 5.6 \times 10^{-10}$	$< 7.5 \times 10^{-10}$
$ q_{\nu_{\mu\tau}} $	$< 1.2 \times 10^{-10}$	$< 1.9 \times 10^{-10}$	$< 2.2 \times 10^{-10}$	$< 3.2 \times 10^{-10}$

Experiment	$q_{\nu_e} [10^{-13} e]$	$q_{\nu_\mu} [10^{-13} e]$	$ q_{\nu_{e\mu}/e\tau} [10^{-13} e]$	$ q_{\nu_{\mu\tau}} [10^{-13} e]$
PandaX-4T	$(-12.6, 16.4)$	$(-22.3, 22.2)$	< 12.2	< 15.7
LZ	$(-4.6, 9.9)$	$(-11.5, 11.3)$	< 6.3	< 8.1
XENONnT	$(-2.5, 7.4)$	$(-8.1, 8.0)$	< 4.4	< 5.7
combined	$(-2.0, 7.0)$	$(-7.5, 7.3)$	< 4.1	< 5.2
DARWIN 30 ty	$(-0.4, 1.0)$	$(-4.1, 4.1)$	< 2.3	< 2.9
DARWIN 300 ty	$(-0.2, 0.4)$	$(-2.4, 2.5)$	< 1.3	< 1.7
DARWIN 300 ty depl.	$(-0.1, 0.3)$	$(-2.2, 2.3)$	< 1.2	< 1.6

Neutrino charge radii

In the Standard Model neutrinos are neutral and there are no electromagnetic interactions at the tree-level

Radiative corrections generate an effective electromagnetic interaction vertex



$$\langle r_{\nu_\ell}^2 \rangle_{\text{SM}} = -\frac{G_F}{2\sqrt{2}\pi^2} \left[3 - 2 \ln \left(\frac{m_\ell^2}{m_W^2} \right) \right]$$

$$\langle r_{\nu_e}^2 \rangle_{\text{SM}} = -0.83 \times 10^{-32} \text{ cm}^2,$$

$$\langle r_{\nu_\mu}^2 \rangle_{\text{SM}} = -0.48 \times 10^{-32} \text{ cm}^2,$$

$$\langle r_{\nu_\tau}^2 \rangle_{\text{SM}} = -0.30 \times 10^{-32} \text{ cm}^2.$$

Neutrino charge radii

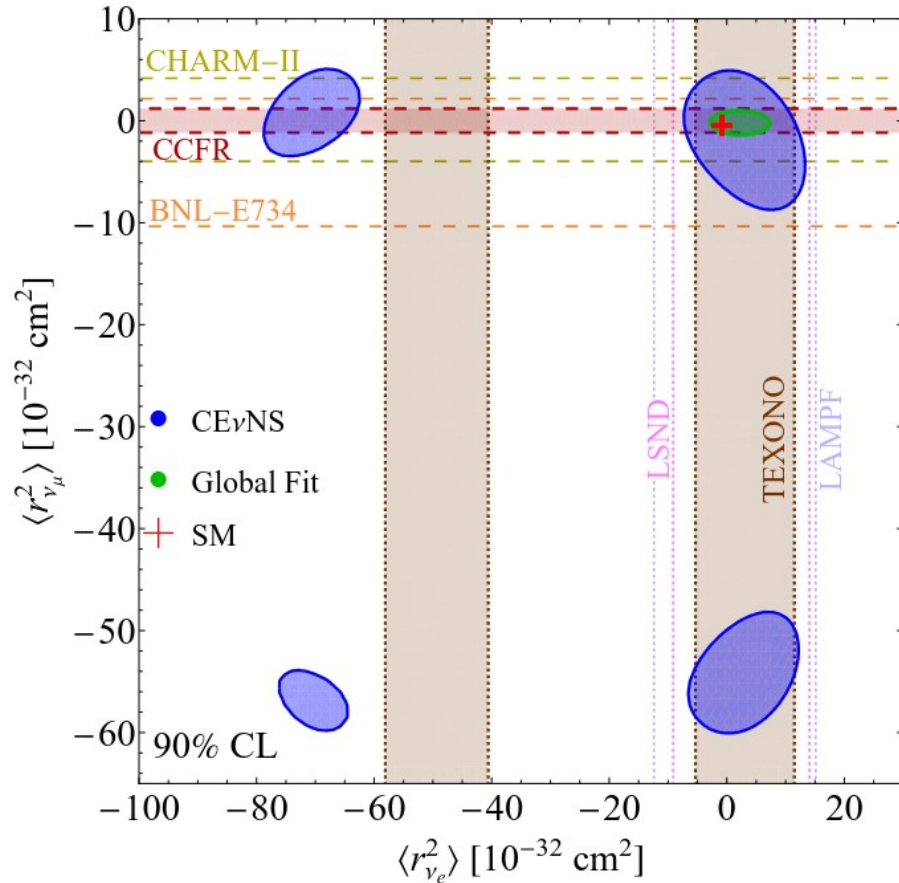
The cross section receives extra contributions which add coherently (diagonal charge radii) and incoherently (non-diagonal charge radii) to the SM cross section

$$\frac{d\sigma_{\nu_\ell - \text{Xe}}^{\text{SM+CR}}}{dT_e} = \left(\frac{d\sigma_{\nu_\ell - \text{Xe}}^{\text{SM+CR}}}{dT_e} \right)_{\langle r_{\nu_\ell}^2 \rangle} + \sum_{\ell' \neq \ell} \left(\frac{d\sigma_{\nu_\ell - \text{Xe}}^{\text{CR}}}{dT_e} \right)_{\langle r_{\nu_{\ell\ell'}}^2 \rangle}$$

$$g_V^{\nu_\ell} \rightarrow g_V^{\nu_\ell} + \frac{\sqrt{2}\pi\alpha}{3G_F} \langle r_{\nu_{\ell\ell'}}^2 \rangle$$

$$\left(\frac{d\sigma_{\nu_\ell - \text{Xe}}^{\text{CR}}}{dT_e} \right)_{\langle r_{\nu_{\ell\ell'}}^2 \rangle} = Z_{\text{eff}}^{\mathcal{A}}(T_e) \frac{\pi\alpha^2 m_e}{9} \left[1 + \left(1 - \frac{T_e}{E_\nu} \right)^2 - \frac{m_e T_e}{E_\nu^2} \right] |\langle r_{\nu_{\ell\ell'}}^2 \rangle|^2$$

Neutrino charge radii



We perform a global fit of the data of many scattering experiments to search for neutrino charge radii

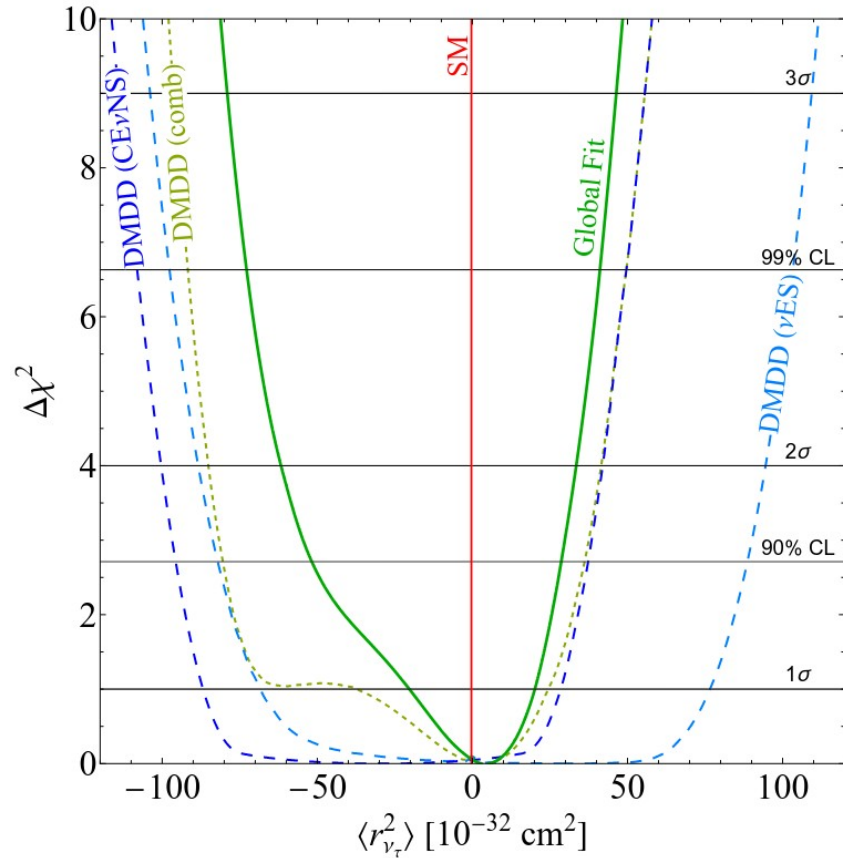
We find

$$\langle r_{\nu_e}^2 \rangle = 2.2_{-2.3}^{+2.4} \times 10^{-32} \text{ cm}^2,$$

$$\langle r_{\nu_\mu}^2 \rangle = -0.19_{-0.56}^{+0.55} \times 10^{-32} \text{ cm}^2$$

Atzori Corona et al, 2504.05272

Neutrino charge radii



The inclusion of DMDD data allows us to bound also the charge radius of ν_τ

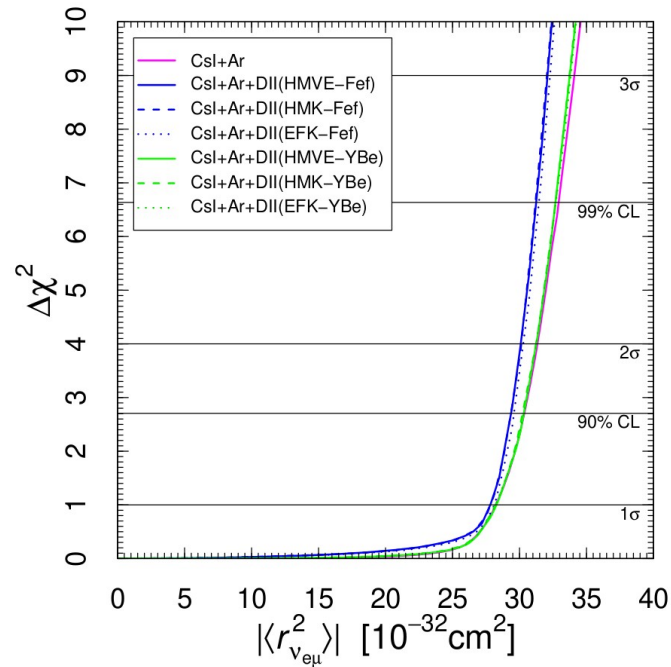
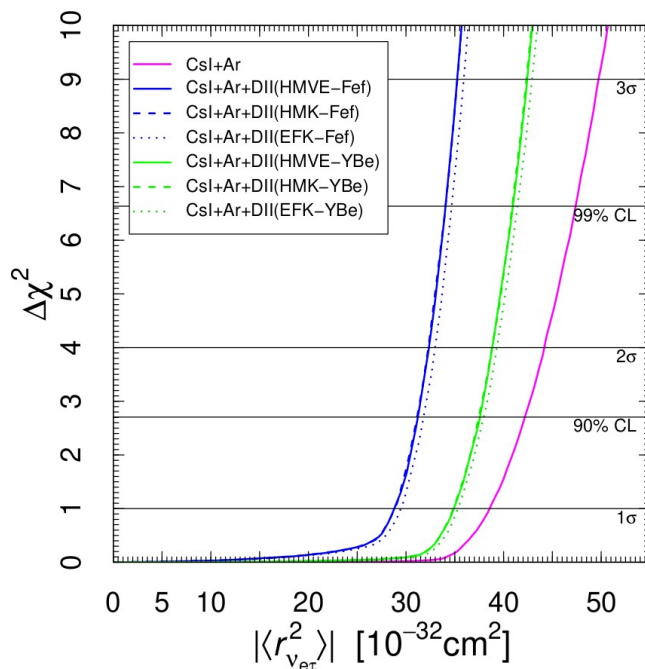
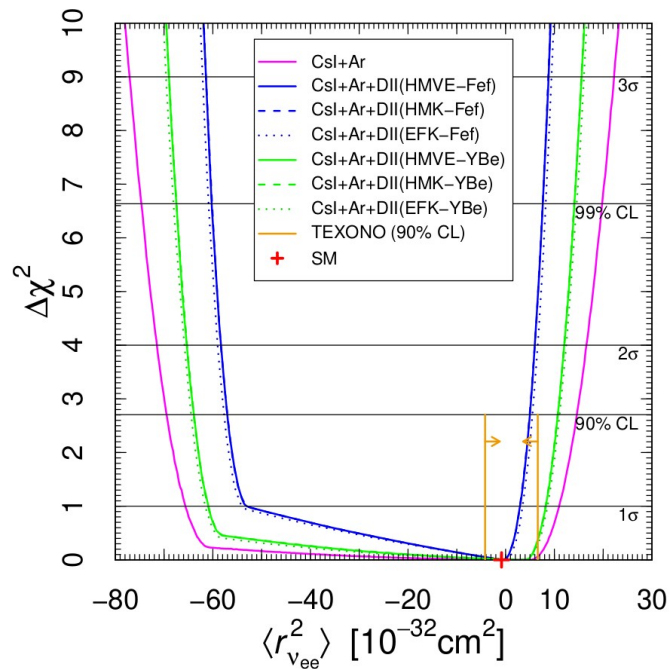
$$-20 \leq \langle r_{\nu_\tau}^2 \rangle [10^{-32} \text{ cm}^2] \leq 20$$

The most stringent constraint on the tau neutrino charge radius obtained from neutrino scattering experiments

Atzori Corona et al, 2504.05272

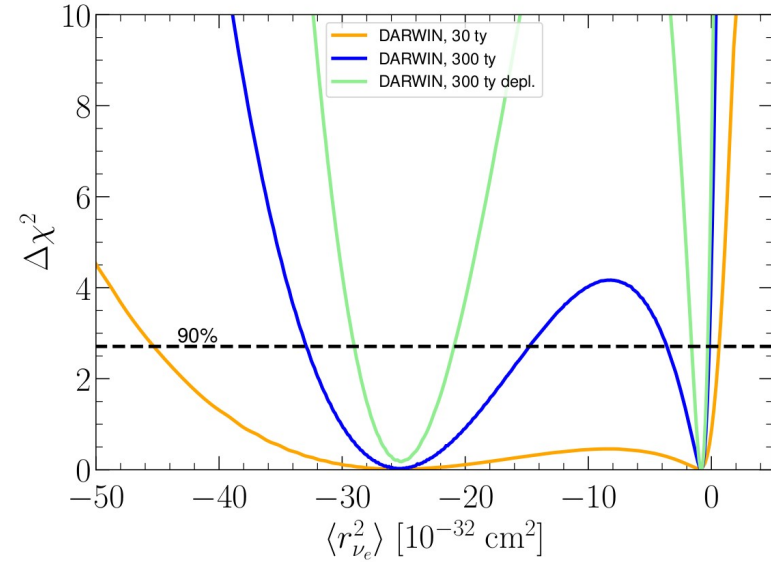
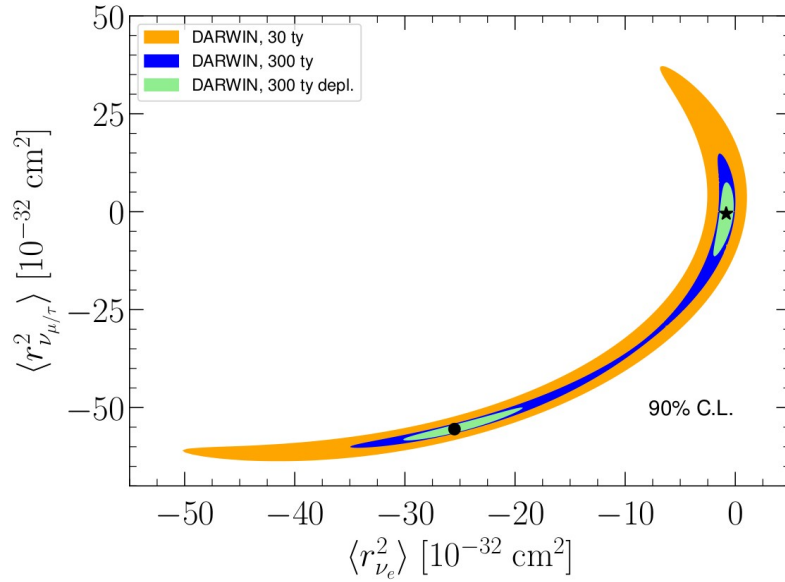
Neutrino charge radii

We also obtain the leading bounds on transition charge radii



Atzori Corona et al, 2205.09484, JHEP 2022

Neutrino charge radii



A measurement of the charge radii could be possible with next generation DMDD detectors!

$\langle r_{\nu_e}^2 \rangle \in (-45.3, 0.6) \times 10^{-32} \text{ cm}^2$, DARWIN 30 ty,
 $\langle r_{\nu_e}^2 \rangle \in \{(-32.9, -14.8) \ \& \ (-3.6, -0.2)\} \times 10^{-32} \text{ cm}^2$, DARWIN 300 ty,
 $\langle r_{\nu_e}^2 \rangle \in \{(-29.1, -20.7) \ \& \ (-1.6, -0.3)\} \times 10^{-32} \text{ cm}^2$, DARWIN 300 ty, depleted

Giunti, Ternes, 2309.17380, PRD 2023

Conclusions

Neutrino scattering experiments provide powerful tools for SM tests and BSM searches

We obtained bounds from EvES and CEvNS data on many potential electromagnetic properties of neutrinos

Some of them (e.g. charge radii) are the most stringent bounds in the literature

DARWIN could provide the first measurement of one of the charge radii

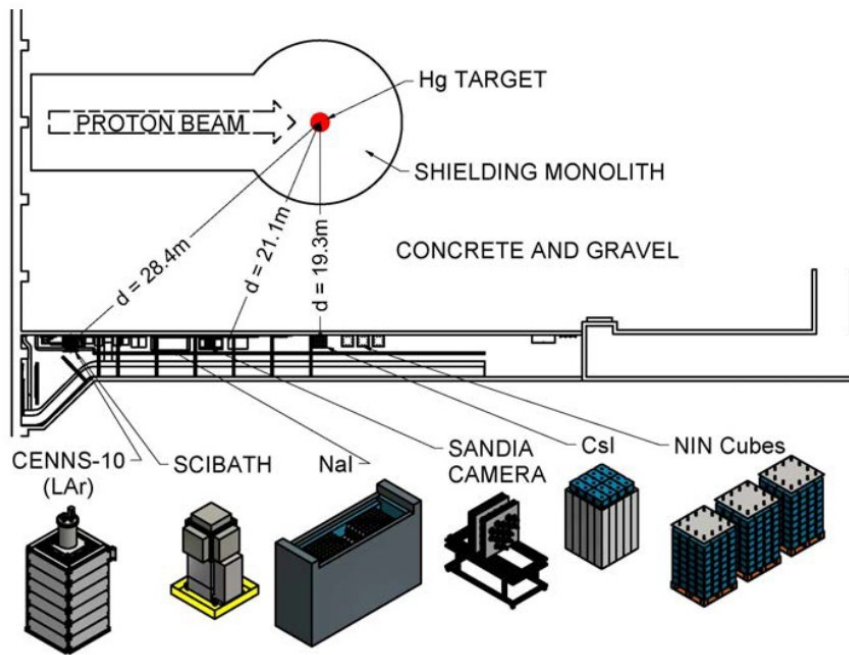
Спасибо!



COHERENT

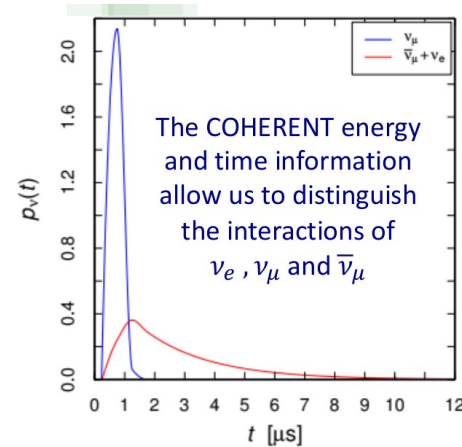
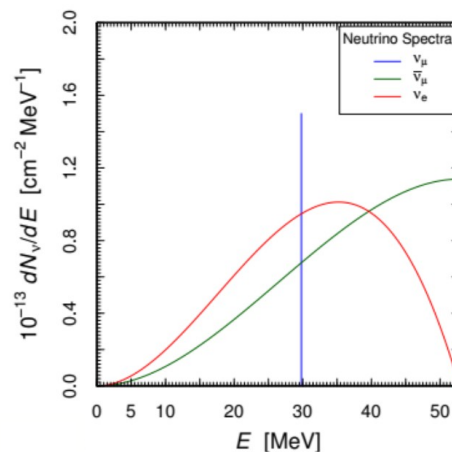
Observed in 2017 in the
COHERENT experiment!

COHERENT uses neutrinos
from the decay of



$$\pi^+ \rightarrow \mu^+ + \nu_\mu$$

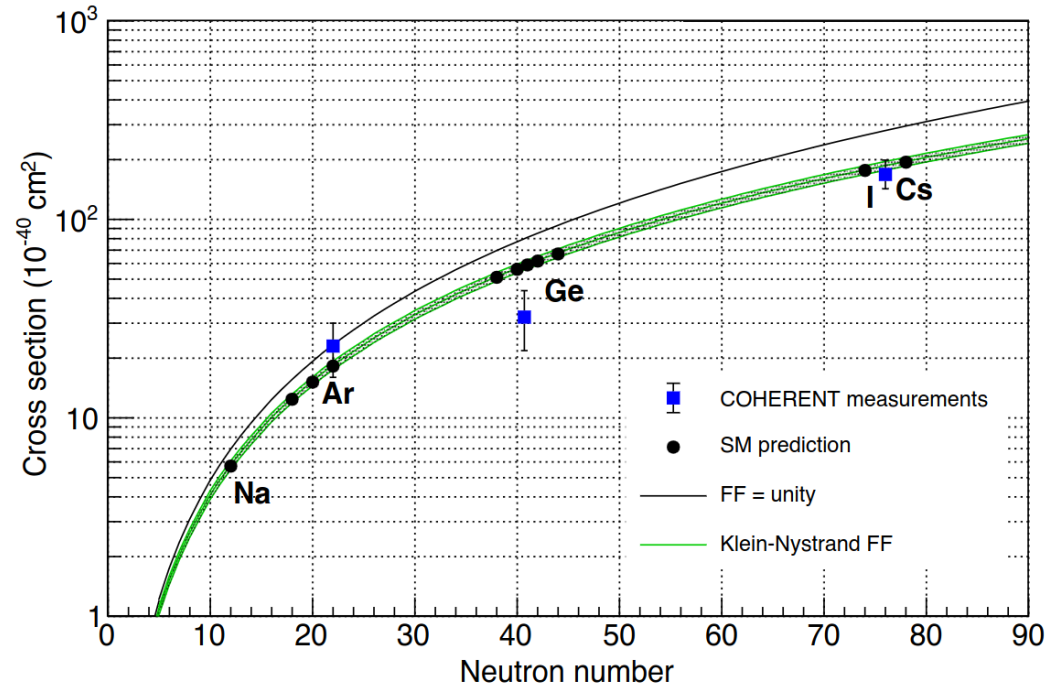
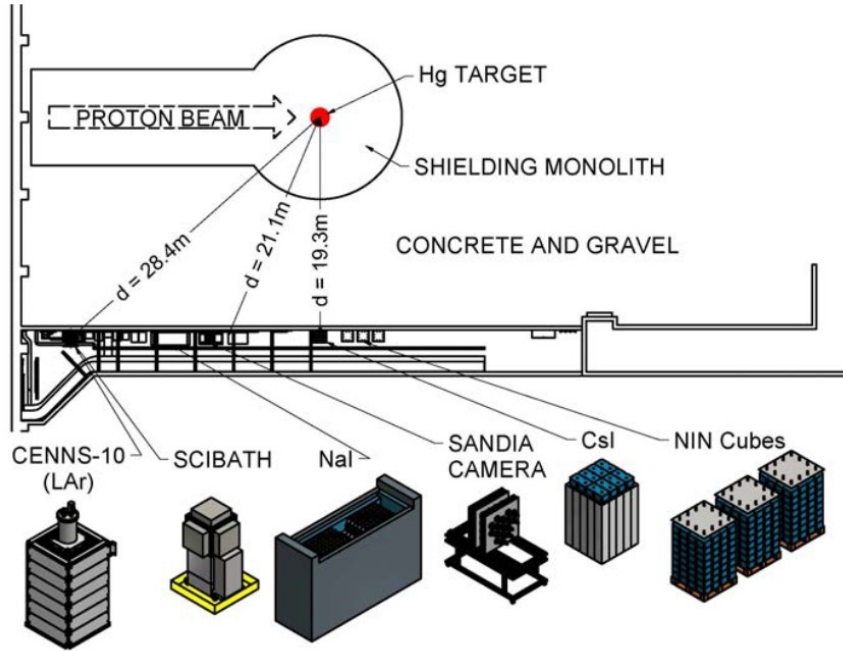
$$\mu^+ \rightarrow e^+ + \nu_e + \bar{\nu}_\mu$$



COHERENT, 1708.01294, Science 2017

Cadeddu et al, 1810.05606, PRD 2018

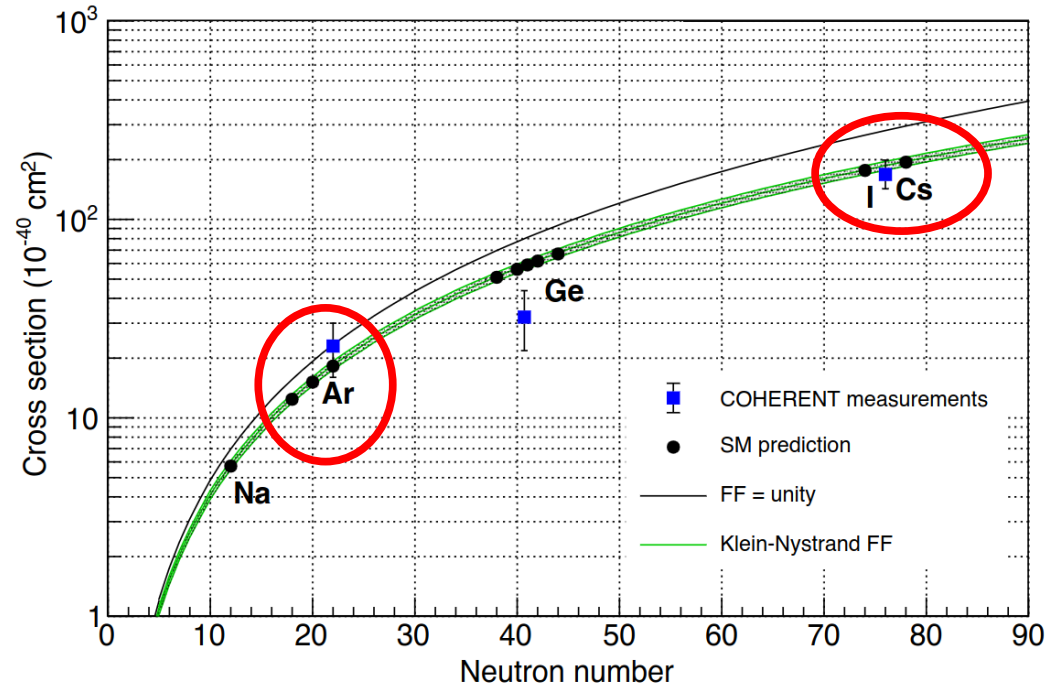
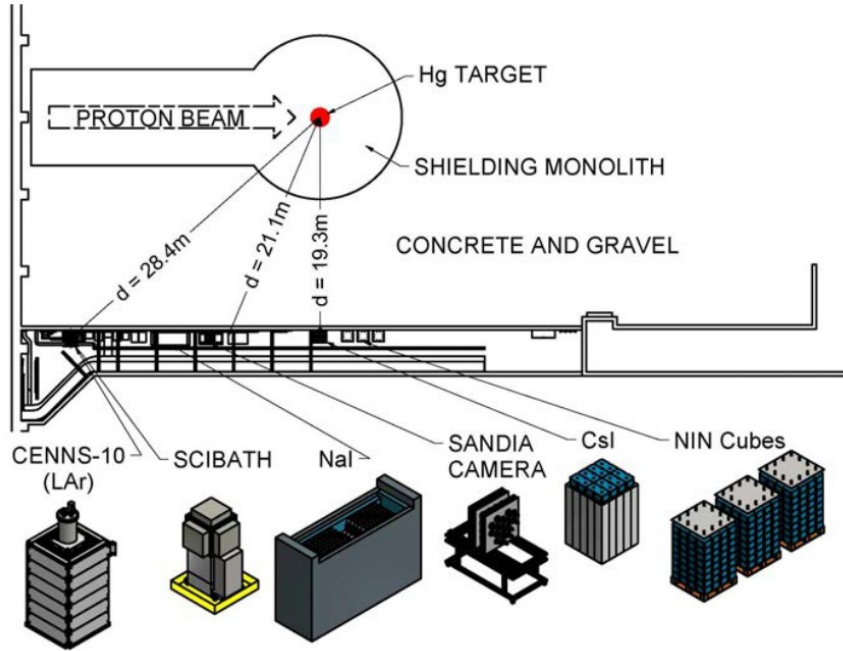
COHERENT



COHERENT, 1708.01294, Science 2017

Mathew Green @ Neutrino-2024

COHERENT



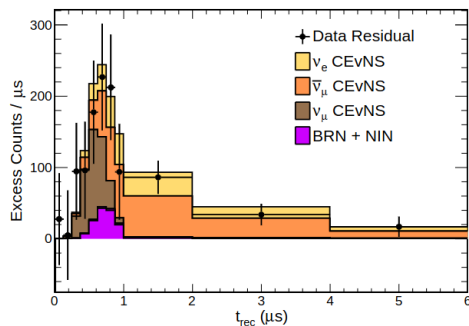
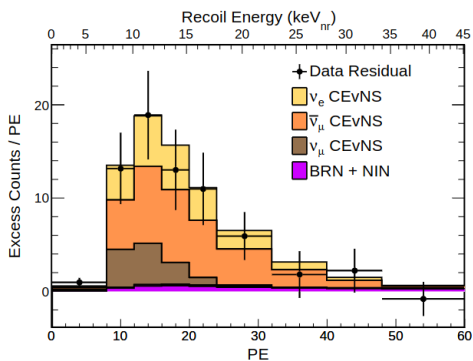
COHERENT, 1708.01294, Science 2017

Mathew Green @ Neutrino-2024

COHERENT

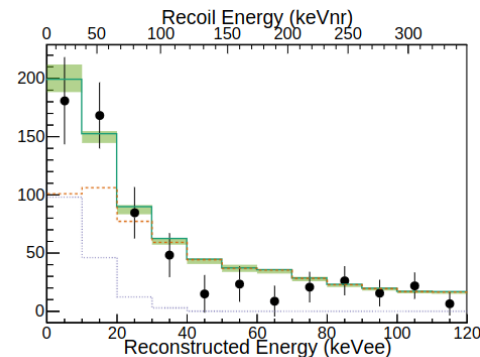
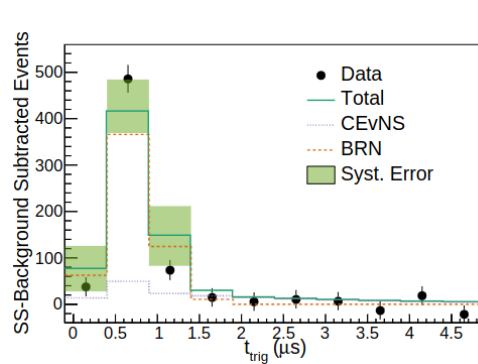
Data included
CEvNS on CsI scintillating crystal

306 ± 20 events, $> 11\sigma$
consistent with SM



COHERENT, 2110.07730, PRL 2022

Data included
CEvNS on liquid argon
Still collecting data, more data
expected to come soon

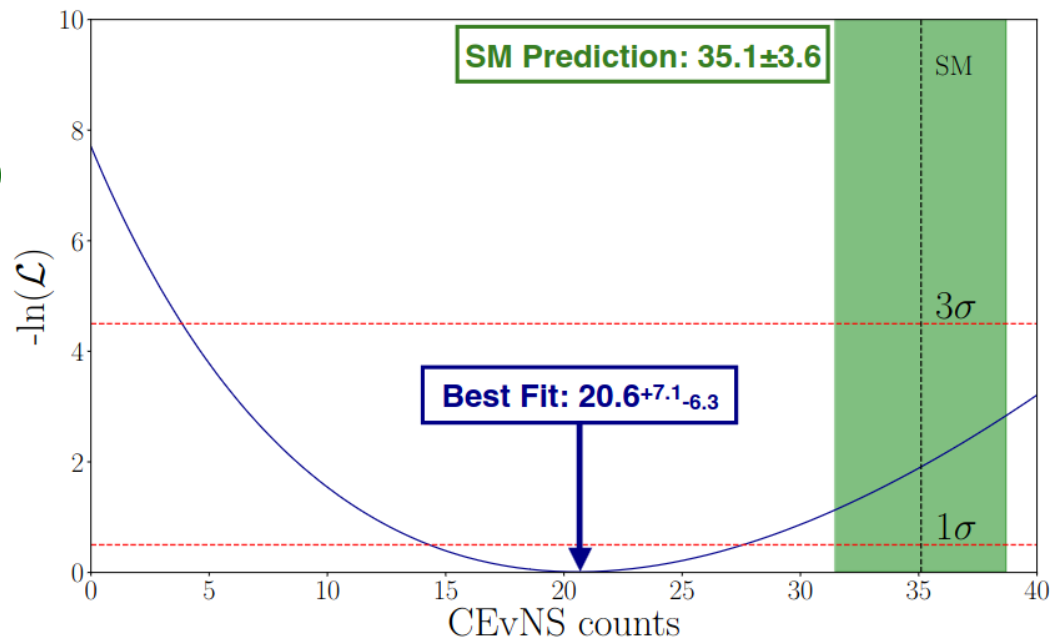


COHERENT, 2003.10630, PRL 2021

COHERENT

New results were presented at the Magnificent CEvNS workshop in Valencia this year!

These data are not included in the analyses discussed today



2D Unbinned Extended Likelihood Fit:

- Null Hypothesis rejected at 3.9 σ
- Reduced χ^2 : 1.84 ($p=0.40$)
- 1.8 σ separation from SM prediction

See:
COHERENT, 2406.13806

COHERENT

Calculation is more complicated

$$N_i^{\text{CE}\nu\text{NS}} = N(\mathcal{N}) \int_{T_{\text{nr}}^i}^{T_{\text{nr}}^{i+1}} dT_{\text{nr}} A(T_{\text{nr}}) \int_0^{T_{\text{nr}}^{\text{max}}} dT'_{\text{nr}} R(T_{\text{nr}}, T'_{\text{nr}}) \int_{E_{\text{min}}(T'_{\text{nr}})}^{E_{\text{max}}} dE \sum_{\nu=\nu_e, \nu_\mu, \bar{\nu}_\mu} \frac{dN_\nu}{dE}(E) \frac{d\sigma_{\nu-\mathcal{N}}}{dT_{\text{nr}}}(E, T'_{\text{nr}})$$

Detector effects (resolution, efficiency, quenching) must be taken into account when calculating the expected number of events

In the statistical analysis we must consider several sources of background and associated systematic uncertainties

$$\chi_{\text{CsI}}^2 = 2 \sum_{i=1}^9 \sum_{j=1}^{11} \left[\sum_{z=1}^4 (1 + \eta_z) N_{ij}^z - N_{ij}^{\text{exp}} + N_{ij}^{\text{exp}} \ln \left(\frac{N_{ij}^{\text{exp}}}{\sum_{z=1}^4 (1 + \eta_z) N_{ij}^z} \right) \right] + \sum_{z=1}^4 \left(\frac{\eta_z}{\sigma_z} \right)^2$$

Atzori Corona et al, 2202.11002, JHEP 2022

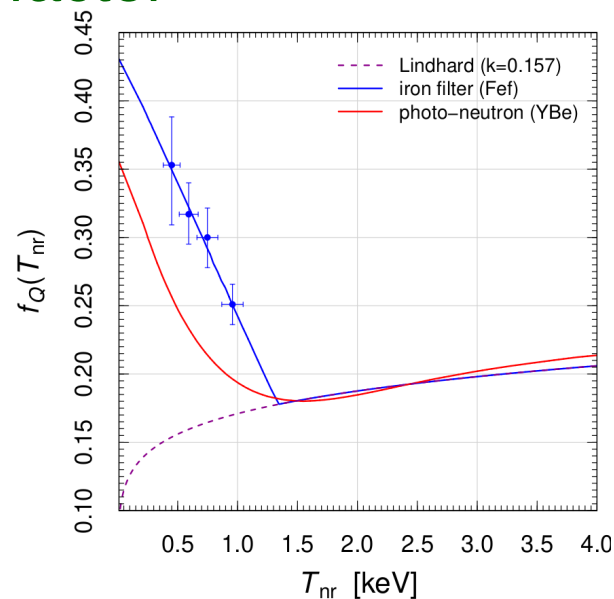
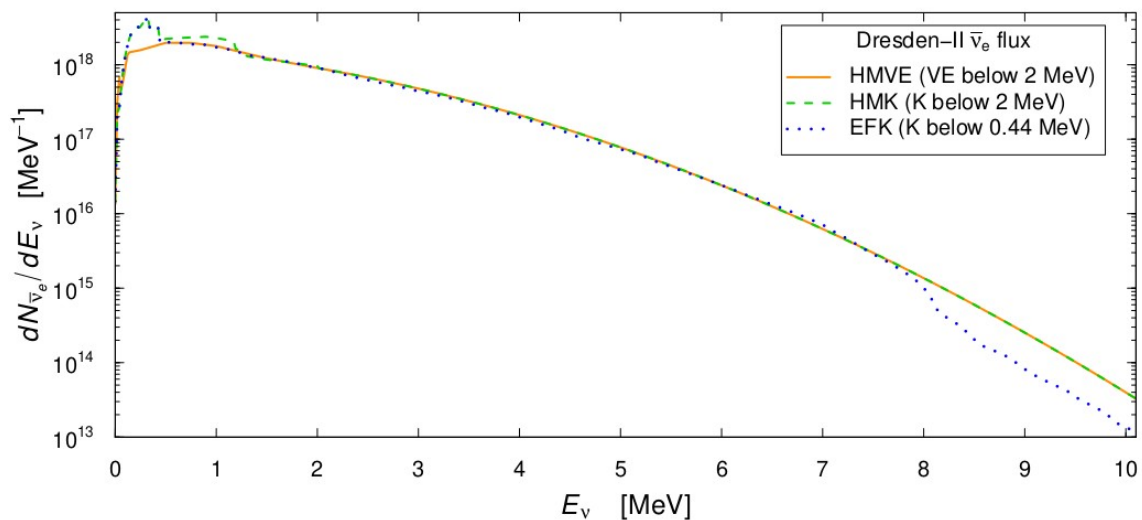
Atzori Corona et al, 2205.09484, JHEP 2022

DRESDEN-II

CEvNS using (anti)neutrinos from a nuclear reactor

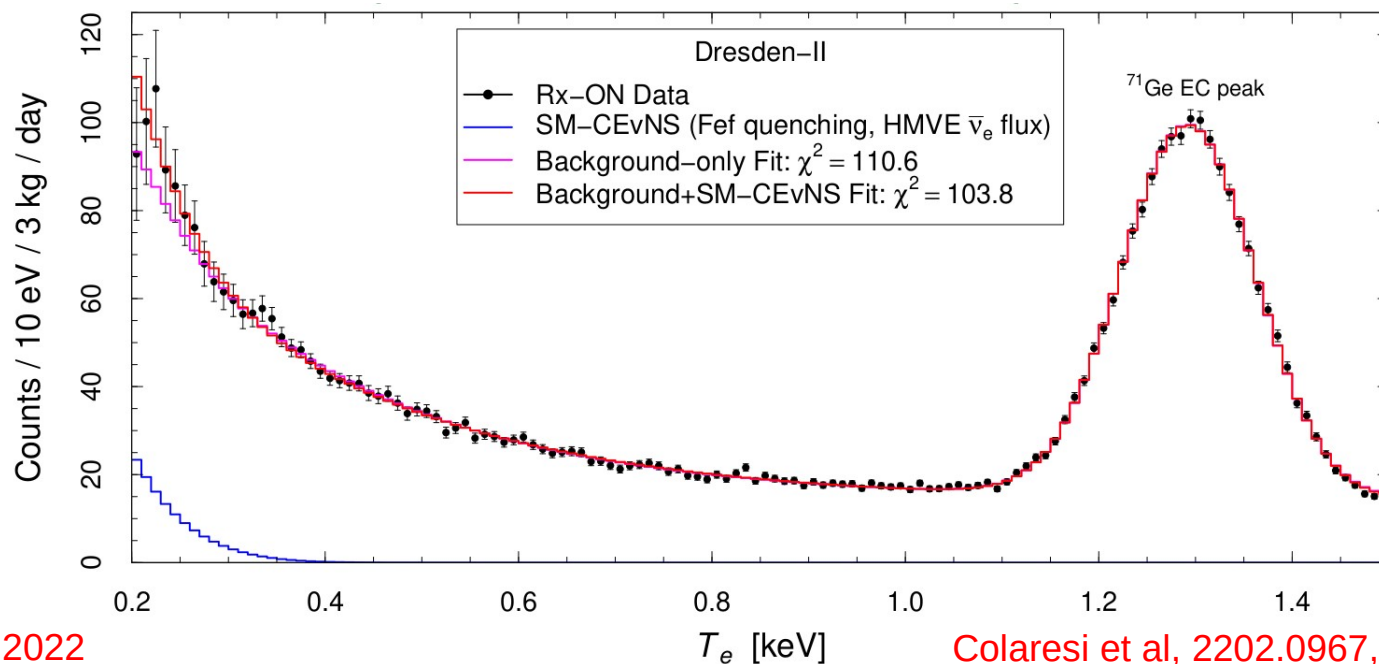
Depends on the reactor flux model under consideration

Depends on the exact form of the quenching factor



DRESDEN-II

Rather CEvNS “indication” than measurement



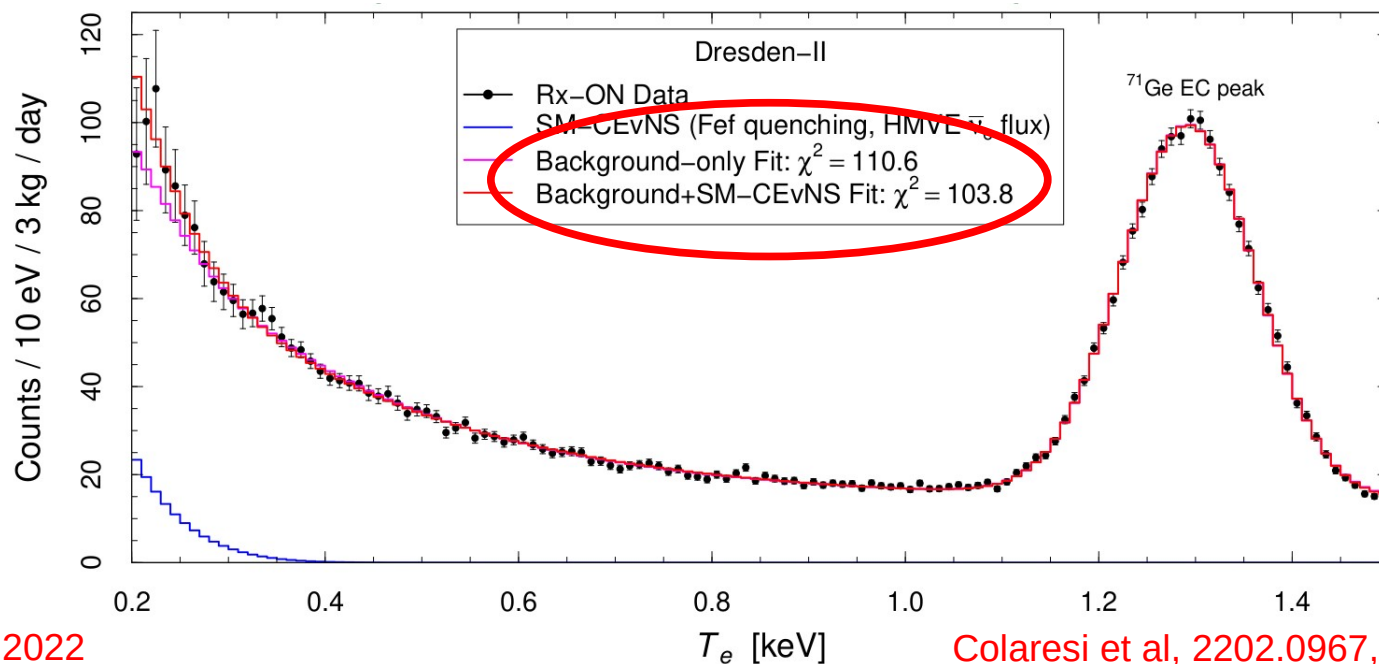
Giunti @ Neutrino 2022

Colaesi et al, 2202.0967, PRL 2022

Christoph Ternes

DRESDEN-II

Rather CEvNS “indication” than measurement



Giunti @ Neutrino 2022

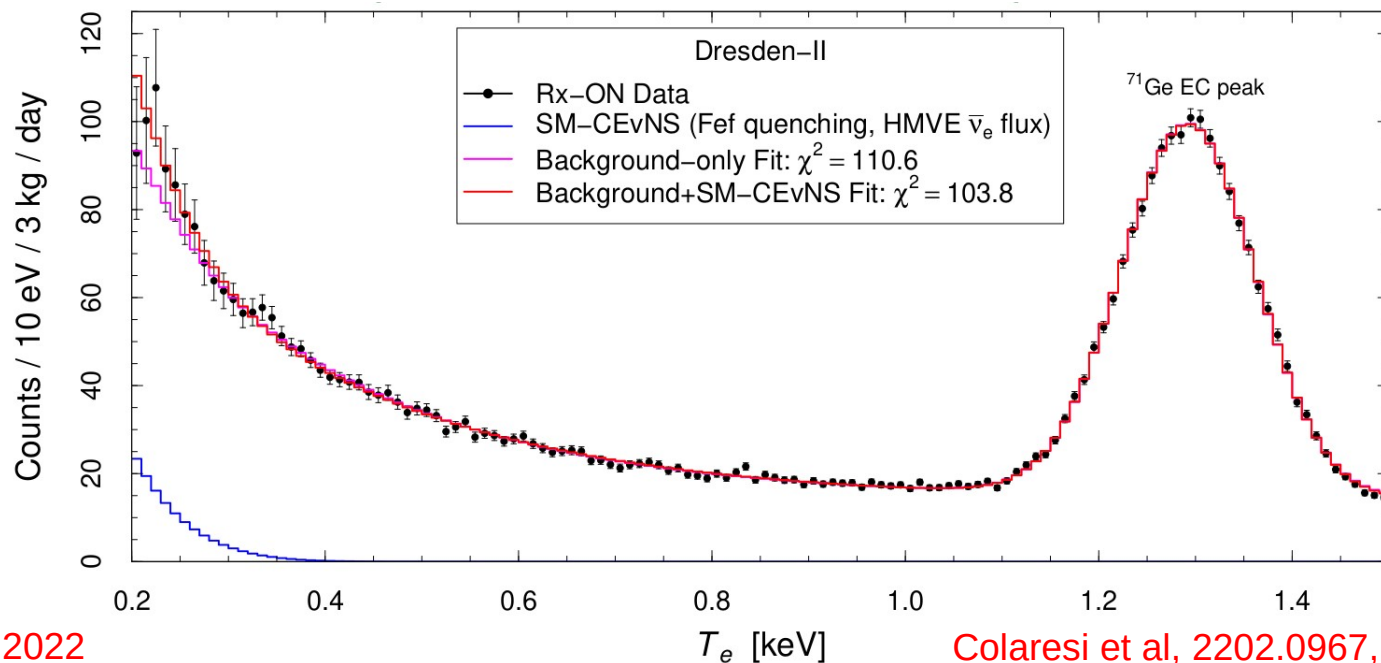
Colaresi et al, 2202.0967, PRL 2022

Christoph Ternes

DRESDEN-II

Rather CEvNS “indication” than measurement

Results debated in the community

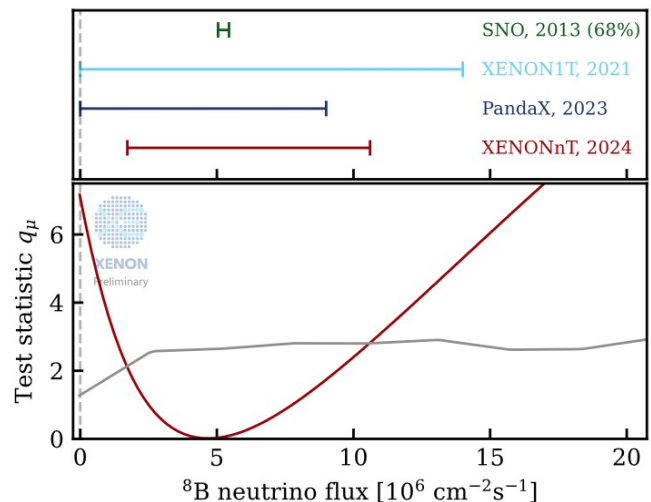


Giunti @ Neutrino 2022

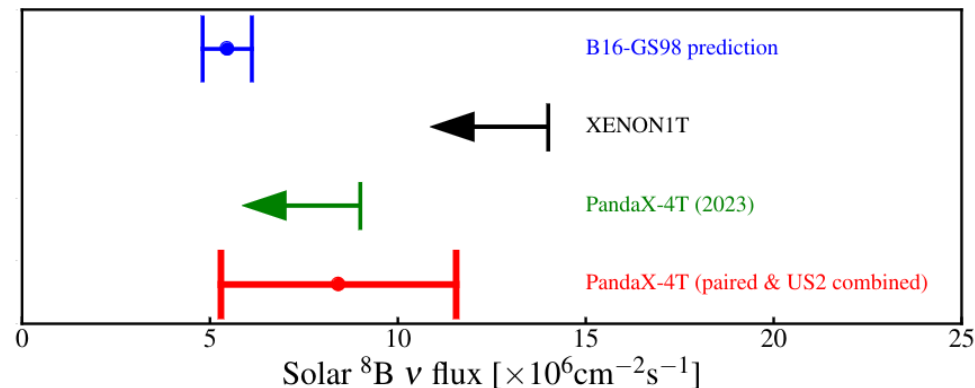
Colaresi et al, 2202.0967, PRL 2022

Christoph Ternes

Dark matter direct detection experiments

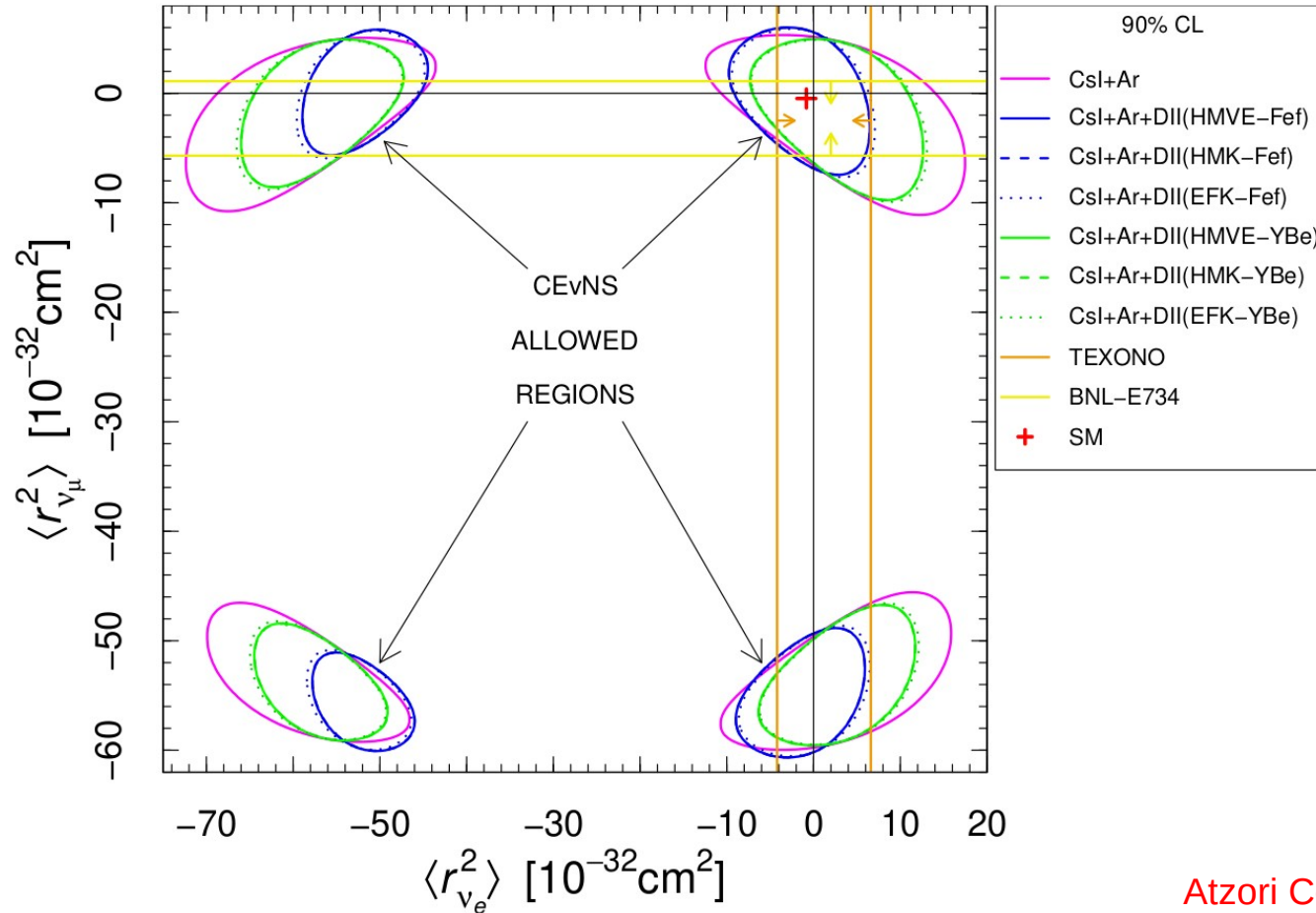


- We have measured the solar ^8B neutrinos via CEvNS in XENONnT at 2.73σ
- The first CEvNS measurement with Xe!
- The first astrophysical neutrino measurement via CEvNS



background-only hypothesis is disfavored at 2.64σ significance.

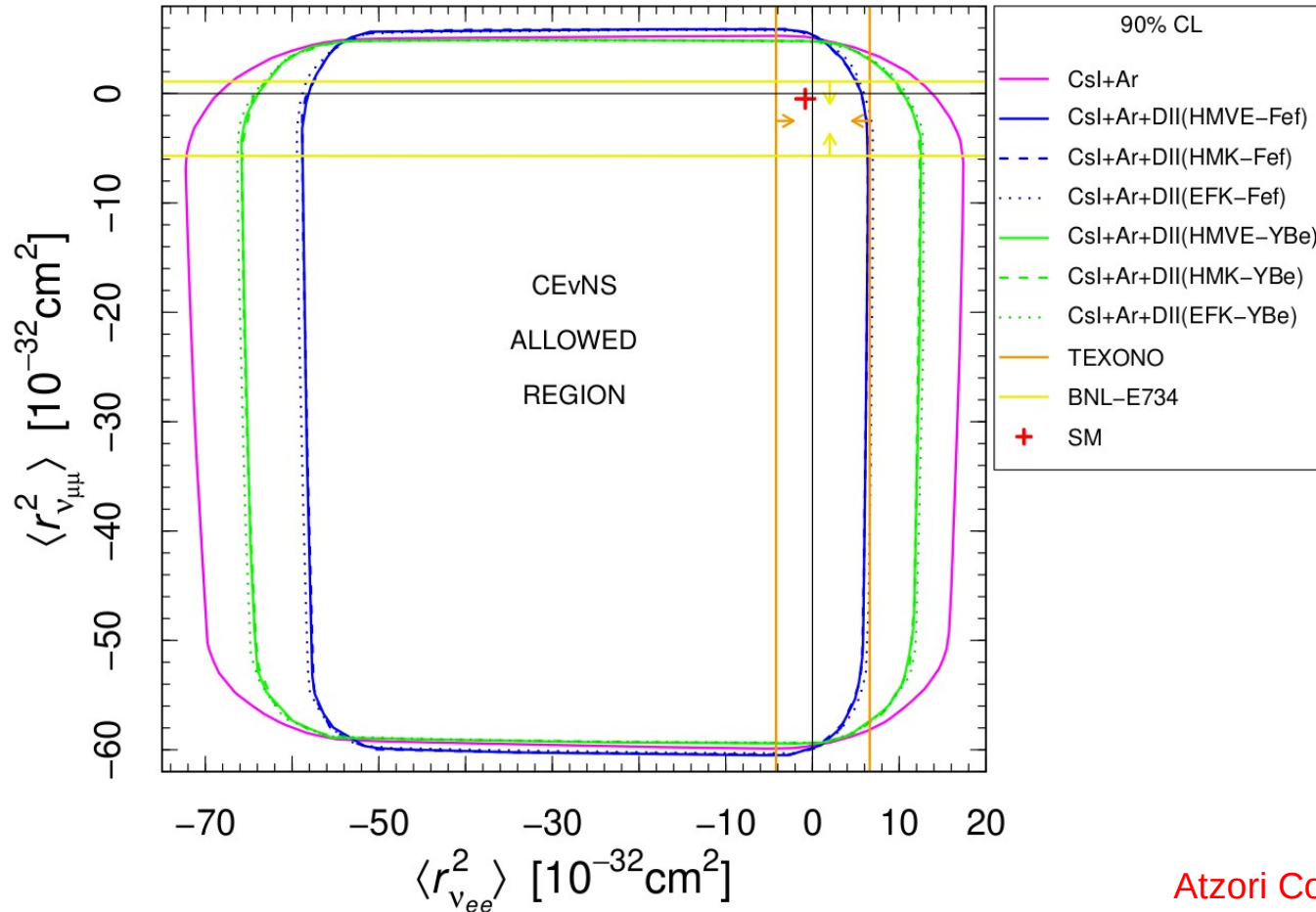
Neutrino charge radii



When allowing only for diagonal elements four separate regions are allowed

Atzori Corona et al, 2205.09484, JHEP 2022

Neutrino charge radii



When allowing only for diagonal elements four separate regions are allowed

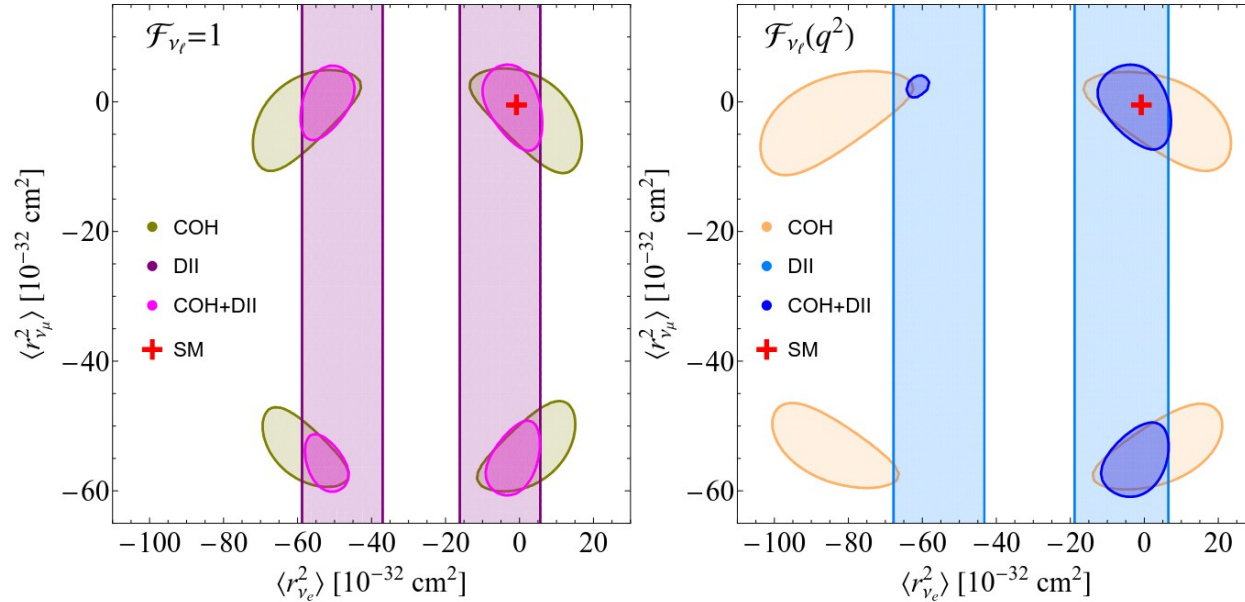
When marginalizing over the non-diagonal parameters the whole interior region remains allowed

Atzori Corona et al, 2205.09484, JHEP 2022

Neutrino charge radii

$$g_V^p(\nu_\ell) = \rho \left(\frac{1}{2} - 2 \sin^2 \vartheta_W \right) + 2\mathbb{X}_{WW} + \mathbb{Q}_{WW} - 2\phi_{\nu_\ell W} + \rho(2\mathbb{X}_{ZZ}^{uL} + \mathbb{X}_{ZZ}^{dL} - 2\mathbb{X}_{ZZ}^{uR} - \mathbb{X}_{ZZ}^{dR})$$

$$g_V^n = -\frac{\rho}{2} + 2\mathbb{Q}_{WW} + \mathbb{X}_{WW} + \rho(2\mathbb{X}_{ZZ}^{dL} + \mathbb{X}_{ZZ}^{uL} - 2\mathbb{X}_{ZZ}^{dR} - \mathbb{X}_{ZZ}^{uR}).$$



Including radiative corrections improves the combined fit

Since they are momentum dependent they affect the COHERENT analysis stronger

Atzori Corona et al, 2402.16709, JHEP 2024